Pulmonary Malformations Beyond the Neonatal Period

Josep M. Mata and Amparo Castellote

Contents

Abstract

Congenital lung malformations are not infrequent. It is necessary to know their radiological manifestations in order to avoid diagnostic errors. We classify the congenital lung malformations into two main groups: Focal malformations and Dysmorphic lung. We review the radiological findings and the role of radiological techniques.

1 Introduction

Congenital lung malformations include a heterogeneous group of anomalies affecting the lung parenchyma, the arterial supply to the lung and its venous drainage (Heitzman 1984). From the morphological-radiological viewpoint, these malformations can be divided into two groups: focal malformations (bronchial atresia, single congenital thoracic cyst, congenital pulmonary airway malformation (CPAM), pulmonary sequestration, and isolated systemic supply to normal lung), and dysmorphic lung (lung agenesis–hypoplasia complex and lobar agenesis–aplasia complex).

2 Focal Malformations

Focal congenital malformations usually involve only a part of the lung. They are a heterogeneous group, whose boundaries are not well defined and whose radiologic and pathologic manifestations vary and can be difficult to classify, especially if infection is present. They may cause symptoms in early life or be discovered incidentally.

Focal congenital malformations can be separated according to their radiologic and pathologic manifestations, with the understanding that significant degrees of overlap may occur. They can be considered a spectrum: at one extreme we find isolated bronchopulmonary anomaly (congenital lobar overinflation: lobar emphysema and bronchial atresia, single congenital thoracic cyst, CPAM);

J. M. Mata (✉)
UDIAT, Servei de Diagnòstic per la Imatge,
Corporació Parc Taulí, Parc Taulí s/n,
08208 Sabadell, Spain
e-mail: jmata@tauli.cat

A. Castellote
Servei de Radiologia Pediàtrica, Hospital Vall d'Hebron,
Ps. Vall d'Hebron 119–129, 08035 Barcelona, Spain

P. Garcia-Peña and R. P. Guillerman (eds.), *Pediatric Chest Imaging*, Medical Radiology. Diagnostic Imaging,
DOI: 10.1007/174_2013_842, © Springer-Verlag Berlin Heidelberg 2013
Published Online: 8 May 2013

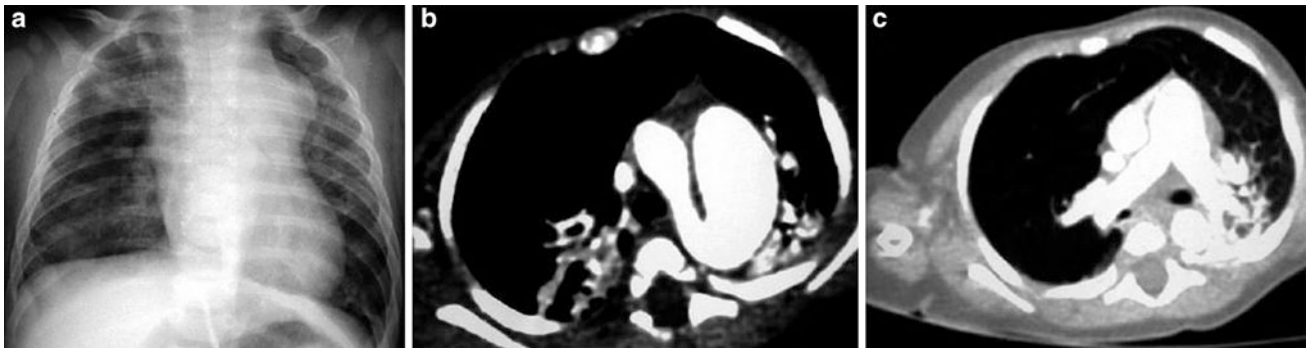

Fig. 1 Patent ductus arteriosus in a 3-month-old girl with pulmonary hypertension. **a** Chest X-ray shows right pulmonary hyperinflation and a bulge in the left upper cardiac silhouette. **b** CT demonstrates that it corresponds to a huge patent ductus. **c** The right main pulmonary bronchus is compressed by the right pulmonary artery causing obstructive emphysema of the right lung

next, associated systemic vascularization in the diseased lung (pulmonary sequestration); and at the other extreme isolated systemic arterial anomalies (isolated systemic supply to normal lung).

Although these developmental lesions usually are isolated, there are too many cases of the concurrent association of two or more of these anomalies, to be on the basis of chance alone. The theory of a variably level, completeness, and timing of the obstruction with secondary pulmonary dysplastic changes may help in understanding this overlap malformations (Langston 2003; Newman 2006).

The prenatal ultrasound (US) and magnetic resonance (MR) examination of the fetus has facilitated recognition and has added new information of many intrathoracic malformations. Nowadays, in countries where fetal US is routinely used, most congenital malformations are discovered antenatally, and confirmed in the neonatal period.

2.1 Congenital Lobar Overinflation: Lobar Emphysema and Bronchial Atresia

2.1.1 Congenital Lobar Emphysema

Congenital lobar emphysema (CLE) is characterized by progressive hyperexpansion of a lobe, usually the left upper or the right middle lobe. Its basic pathologic abnormality is overdistension of otherwise normal alveoli without destruction of alveolar walls. Proposed etiologies include focally deficient bronchial wall cartilage, deficient connective tissue stroma resulting in abnormal support of alveolar walls, and intrinsic or extrinsic obstruction of an affected bronchus. These abnormalities are believed to result in a check-valve mechanism, with progressive hyperinflation of the involved lobe after birth. Infrequently, lobar emphysema can be acquired. It can be caused by extrinsic compression from a vascular anomaly such as an enlarged pulmonary artery or vein (Figs. 1, 2), a patent ductus arteriosus or a mediastinal mass (Winters and Effmann 2001). Clinically, most infants with CLE present within the first 6 months of life, with symptoms and signs of respiratory distress. Radiographs obtained beyond the neonatal period always demonstrate hyperlucency and overexpansion of the affected lobe and variable degrees of atelectasis of the ipsilateral lobe or lobes with associated mediastinal shift. CT is useful to exclude other causes of lobar emphysema, such as vascular anomalies or a mediastinal mass. CT findings of CLE are an expanded hemithorax, an overinflated low-attenuation lobe with stretching and attenuation of the pulmonary vessels, and atelectasis of the adjacent lobes. The paucity of vascular shadows within the overexpanded lung is in itself diagnostic of obstructive emphysema. Expiratory slices will confirm severe air-trapping in the affected lobe. Follow-up scans of patients who have minimal or no symptoms and, therefore, are treated conservatively, usually demonstrate either no changes or a progressive reduction in the degree of overexpansion of the affected lobe. However, significant air-trapping on expiration persists. Bilateral or multifocal involvement is rare (Hugosson et al. 1995).

2.1.2 Bronchial Atresia

Bronchial atresia (BA) is an anomaly characterized by obliteration of the proximal lumen of a segmental bronchus, with preservation of the distal structures. Its pathogenesis is unknown, although it may be due to a vascular insult. Most pediatric BA cases are congenital, but the condition may be acquired secondary to traumatic or infectious injury to the bronchus (Wasilewska et al. 2012). Air enters the affected segment via collateral channels, producing overinflation and air-trapping. The mucus secretions generated in the bronchi accumulate at the point of obstruction, originating mucus impaction (Lemire et al. 1970; Felson 1979). The mucocele can be linear, branched, ovoid, or spherical. BA almost always affects just one segment, and rarely affects a lobar

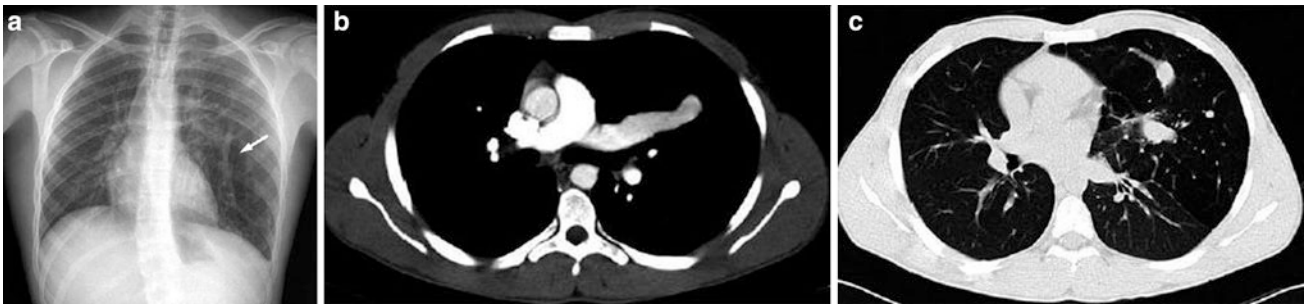

Fig. 2 17-year-old boy with chest pain. **a** Chest radiograph shows a hyperinflation of the lingula and a vascular linear shadow (*arrow*) **b**, **c** CT demonstrates that this structure corresponds to a huge single pulmonary vein going to the left atrium. Hyperinsuflation of the lingula is also seen

Fig. 3 Bronchial atresia in a 17-year-old girl. Expiratory CT image with lung window shows the bronchocele and hyperinflation of the right upper lobe

Fig. 4 Bronchial atresia in a 4-year-old boy. CT scan imaged with lung window shows a cystic lesion containing gas and fluid at the right hilum (*arrow*) corresponding to the dilated right upper lobe bronchus and hyperinflated right upper lobe

bronchus. Involvement of multiple segments has been reported in a few cases (Ward and Morcos 1999). BA is characteristically located in the left upper lobe (apico-posterior segment), but can involve any lobe (Remy-Jardin et al. 1989; Medelli et al. 1979) and can be associated with other congenital anomalies. It is usually asymptomatic and is an incidental finding on radiological study. Infection of the unconnected lung is rare.

The chest plain film usually demonstrates pulmonary insufflation with trapped air during expiration, accompanied by a tubular, branched, or spherical image in a central position, which corresponds to the mucocele (Jederlinic et al. 1986). CT shows the segmental overinflation and mucous impaction with great precision. When BA does not involve the left upper lobe or when it does not present characteristic radiological findings in the plain film, CT is diagnostic, demonstrating the combination of emphysema and bronchial impaction that is the hallmark of this condition (Pugatch and Gale 1983; Finck and Milne 1988) (Fig. 3). In some cases, a cystic lesion containing gas and fluid corresponding to a severely dilated bronchus just distal to segmental bronchial atresia can also be seen (Griscom 1993) (Fig. 4).

When the mucocele cannot be identified, radiological diagnosis of bronchial atresia versus CLE may be impossible. In both these entities symptoms may be absent and radiological features may progressively improve. Nonetheless, the degree of mediastinal shift and collapse of the ipsilateral lobes is much more significant in most cases of lobar emphysema than in bronchial atresia (Castellote et al. 2005).

MRI is not commonly used to evaluate bronchial atresia after birth, but this malformation can be depicted on prenatal MRI. The obstructed lobe appears hyperintense on T2-weighted images. This appearance can also be seen in CLE, type III CPAM, and BPS (Recio Rodríguez et al. 2012; Biyyam et al. 2010).

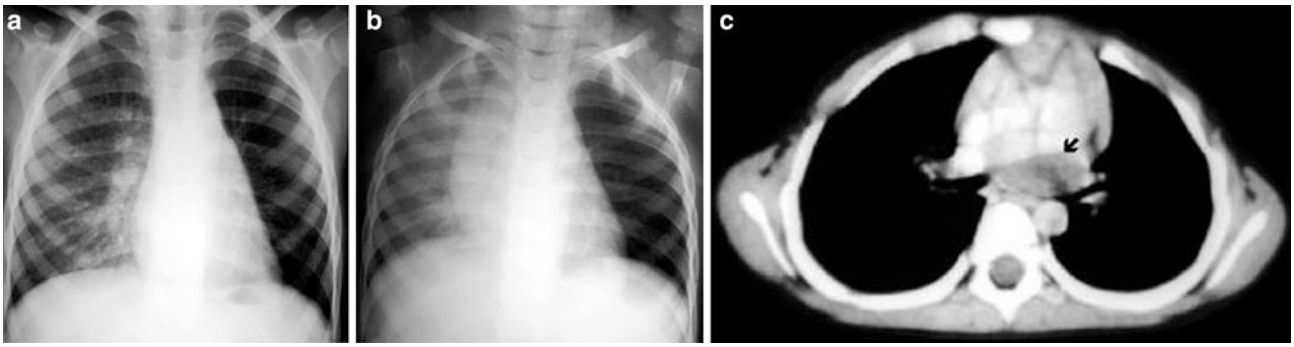

Fig. 5 Bronchogenic cyst in a 3-year-old boy. **a** Inspiratory chest radiograph shows hyperlucency and decreased vascular perfusion in the left lung. **b** Expiratory chest radiograph demonstrates air-trapping in the left lung. **c** A subcarinal cyst compressing the left main bronchus is seen in the CT scan (*arrow*)

2.2 Single Congenital Thoracic Cyst

We include under the term single congenital thoracic cyst (SCTC) all congenital cysts located in the mediastinum (bronchogenic cysts, duplication cysts, and pleuropericardial cysts) and lung parenchyma. Treatment of SCTC depends on the symptoms. The best approach in asymptomatic patients with mediastinal cysts is periodic control, avoiding surgery. For practical purposes of clinical management, all cysts located within the lung parenchyma can be considered bronchogenic cysts requiring surgery. The definitive diagnosis of SCTC should be established on the basis of the study of the cyst wall. When there is associated inflammation and in some cases of mediastinal cysts, diagnosis can be difficult.

The most frequent location of bronchogenic cyst varies according to the published series (DuMontier et al. 1985; Baker 1989; Patcher and Lattes 1963; Rogers and Osmer 1964). In the most recent series including 68 bronchogenic cysts (McAdams et al. 2000), 58 (85 %) were mediastinal, and seven were intrapulmonary (10 %), demonstrating a clear predominance of mediastinal cysts. Mediastinal cysts are most often found in a subcarinal location, whereas intrapulmonary bronchogenic cysts are most frequently located in the lower lobes. Bronchogenic cysts can be found in the diaphragm, below the diaphragm (Braffman et al. 1988) and even in the liver (Kimura et al. 1990) or neck and can be associated with pericardial agenesis (Kwak et al. 1971). They are usually solitary and spherical in shape with thin walls of bronchial epithelium, and have a viscous gelatinous, mucoid, hemorrhagic or watery, translucent fluid content. They occasionally contain calcium, have calcified walls, or are completely calcified and they can be air-filled when they communicate with the bronchial tree (Rogers and Osmer 1964; Reed and Sobonya 1975). Bronchogenic cysts are sometimes found in association with other congenital pulmonary malformations such as sequestration, lobar emphysema, or BA (Kuhn and Khun 1992; Grewal and Yip 1994).

In infants mediastinal SCTC tend to compress or distort the esophagus, the trachea, and bronchi, resulting in clinical respiratory compromise, but the condition can be asymptomatic and be discovered fortuitously. Compression of a main bronchus may result in obstructive pulmonary hyperinflation of the ipsilateral lung (Fig. 5). These cysts can also compress the pulmonary artery or superior vena cava (Bankoff et al. 1985). Mediastinal and intrapulmonary SCTC can disappear spontaneously (Martin et al. 1988), change form due to decreases in their internal pressure, or diminish in size, making themselves invisible to the chest plain film (Fig. 6).

The basic radiological study used to detect SCTC is the chest plain film. In the majority of cases, this technique detects the lesion and some of the complications (e.g., compression on neighboring structures). Ultrasound, MDCT, and MR allow a better evaluation of SCTC and its anatomic relationship with adjacent structures. CT reveals a round or ovoid mass with water or soft-tissue attenuation. Almost 50 % of SCTC appear iso- or even hyperdense at CT due to intracystic hemorrhage, protein content, or milk of calcium. On MRI, SCTC are homogeneously and markedly hyperintense on T2-weighted images. The intracystic signal intensity on T1-weighted images is more variable, and, depending upon the cyst content, low, intermediate, and high signal intensity cases have been reported (Naidich et al. 1988; Nakata et al. 1993). Relatively high signal intensity on T1 is due to a high protein content and or the presence of methemoglobin. Fluid–fluid levels have also been reported (Lyon and McAdams 1993). When air–fluid levels are seen within the cyst, it is usually infected, although we have seen cysts with air–fluid levels in asymptomatic patients (Fig. 7). Minimal wall enhancement is expected with gadolinium enhancement.

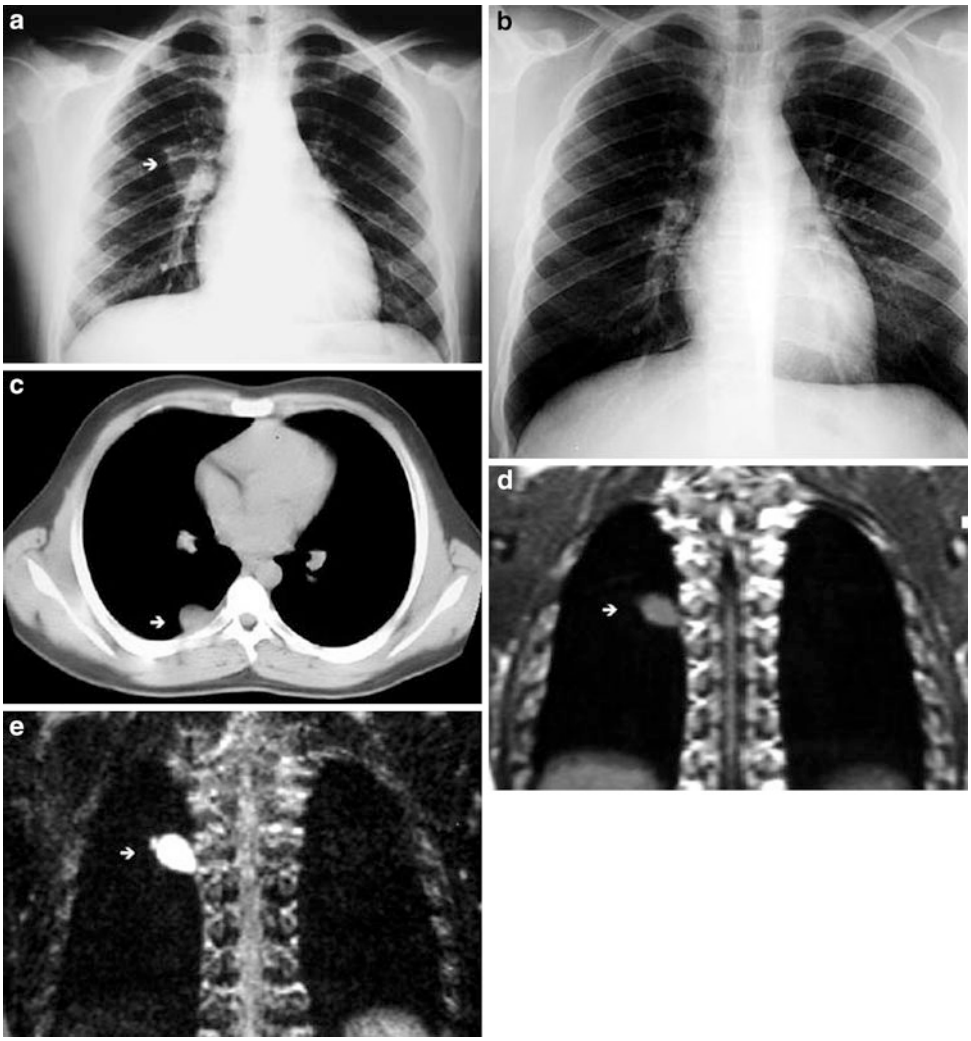

Fig. 6 Mediastinal bronchogenic cyst in a 14-year-old boy. **a** Chest radiograph shows an ovoid perihilar mass in the right upper lobe (*arrow*). **b** Chest radiograph performed 1 year later, prior to surgery, is normal. **c** CT scan performed at the same time as (**b**), shows an isodense mass in the right upper lobe (*arrow*). **d** Coronal T1-weighted MR image demonstrates the presence of an intermediate signal intensity ovoid mass (*arrow*). **e** Coronal T2-weighted MR image. The homogeneous high signal intensity of the mass indicates a fluid content (*arrow*)

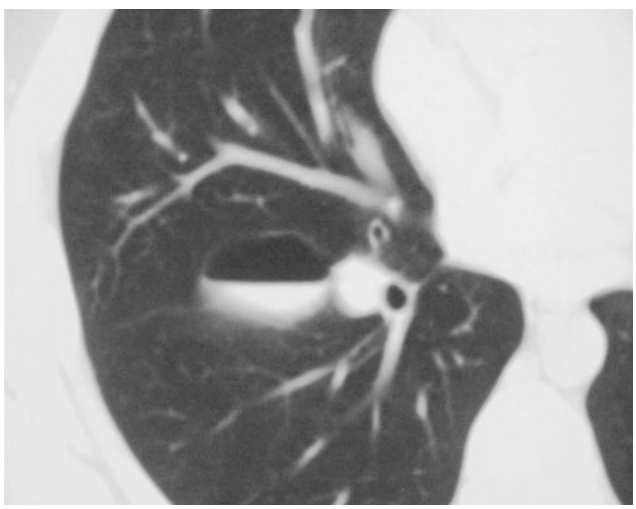

Fig. 7 Bronchogenic cyst in an asymptomatic 12-year-old boy. CT scan shows an air–fluid level within the cyst

2.3 Congenital Pulmonary Airway Malformation: Pulmonary Sequestration Complex

2.3.1 Congenital Pulmonary Airway Malformation

Congenital pulmonary airway malformation, previously named congenital cystic adenomatoid malformation (CCAM) consists of an intrapulmonary mass of disorganized pulmonary tissue that may or may not be accompanied by macroscopic cysts (Stocker 2002). When present, the cysts communicate with the airways and their vascular supply comes from pulmonary circulation. However, there are numerous examples of CPAM fed by systemic blood vessels and in these cases it is extremely difficult to differentiate CPAM from pulmonary sequestration, as they correspond to overlapping malformations (Winters et al. 1997). From the radiological viewpoint the differentiation between CPAM with systemic supply and pulmonary sequestration is impossible. These malformations correspond to the same

Table 1 The extended classification of congenital pulmonary airway malformation

Type	Incidence (%)	Gross appearance	Microscopy	Other features
0	1–3	Solid; both lungs are small and firm	Bronchial-type airways that have cartilage, smooth muscle, and glands are separated by abundant mesenchymal tissue	Incompatibility with life
1	60–70	Large cysts (up to 10 cm)	The cysts are lined by pseudostratified ciliated cells that are often interspersed with rows of mucous cells	May be late; best overall prognosis; less than 1 % carcinomatous change
2	10–15	Sponge-like composed of multiples cysts (up to 2 cm) and solid pale tumor-like tissue	The cysts resemble dilated bronchioles separated by normal alveoli; striated muscle in 5 %	Neonates; cardiac and renal anomalies; poor prognosis
3	5	Solid	Scattered bronchiolar/alveolar duct-like structures are lined by low cuboidal epithelium and surrounded by alveoli lined by cuboidal epithelium	Neonates, almost exclusively in males; poor prognosis
4	15	Large cysts (up to 10 cm) generally at the periphery of the lung	The cysts are lined by a flattened epithelium resting on loose mesenchymal tissue	Neonates and infants; good prognosis; overlap with PPB

Adapted from Macsweeney et al. (2003)

clinical and radiological entity, although they have a different anatomo-pathological expression.

Ch'in and Tang applied the name "congenital cystic adenomatoid malformation" to a congenital cystic pulmonary anomaly for the first time in 1949. The essential discovery is an adenomatoid proliferation of the terminal bronchioles that produces cysts of varying sizes coated with bronchial epithelium. There is considerably controversy over classification and nomenclature. CPAM has recently been recommended as a preferred term to congenital cystic adenomatoid malformation because not all the lesions are cystic and only type III is adenomatoid. In 1977 Stocker et al. divided CCAM into three groups, depending on whether the cysts were larger than 2 cm (type I), smaller than 2 cm (type II), or the malformation was solid without cysts (type III). (Stocker et al. 1977). An expanded classification (types 0–4) has been proposed representing malformations of larger through smaller airways. In an attempt to maintain a similar ordering of the three types published in 1977, type I, II, and III become type 1, 2, and 3 and the "distal acinar" lesion added is type 4, presenting features of a large cyst generally located at the periphery of the lung. Type 0 is characterized by its involvement of all lobes of the lung and its incompatibility with life (Table 1). A number of reports have been suggesting a relationship between CPAM and pleuropulmonary blastoma (PPB) and it is unclear at this time. Anyway, although Stocker feels based in his experience that they are separate lesions, other authors (MacSweeney et al. 2003) consider that both lesions show histologic overlap.

CPAM can be associated with other congenital malformations such as pulmonary sequestration, tracheal bronchus, tracheal atresia, tracheal diverticulum (Restrepo et al. 2004), and bronchogenic cyst. CPAM can also be associated with congenital BA in the same lobe (Cachia and Sobonya 1981) or can involve more than one lobe or be bilateral. In our experience it occurs with more frequency in lower lobes. CPAM can cause severe respiratory distress in the neonatal period. Beyond this time it is usually discovered when it becomes infected or as an incidental radiological finding (Pulpeiro et al. 1987).

The malformation can escape detection on plain films. Although, these days, however, CPAM is increasingly being diagnosed on antenatal (US) examinations, where it is seen as an echogenic mass, which may or may not contain cysts. Antenatal MR imaging may help to evaluate any associated pulmonary hypoplasia and predict the prognosis. The lesions may disappear completely, may remain unchanged or increase in size and be associated with the development of polyhydramnios or fetal nonimmune hydrops fetalis (Fig. 8) (Paterson 2005).

The appearance of CPAM on radiographs and CT depends on the relative presence of cystic and solid components and whether there is superimposed infection. On plain films, type I presents as one or more dominant cysts with adjacent smaller cysts and solid tissue elements. Type II displays smaller, more evenly sized and spaced cysts. Type III, which is very rare, appears as a solid mass. Large masses produce significant mediastinal displacement. Air-fluid levels are often seen, mainly, but not always, associated with infection. On chest CT, CPAM is seen as multiple thin- or thick-walled, air- or fluid-filled cysts of variable size, expanding the affected lung. Air-fluid levels are often present (Rosado-de-Christenson and Stocker 1991). CPAM may mimic cystic pleuropulmonary blastoma. PPB is probably the same tumor that several authors have reported as mesenchymal sarcoma or rhabdomyosarcoma arising in congenital lung cysts (Ueda et al. 1977). It has also been stated that PPB can arise from

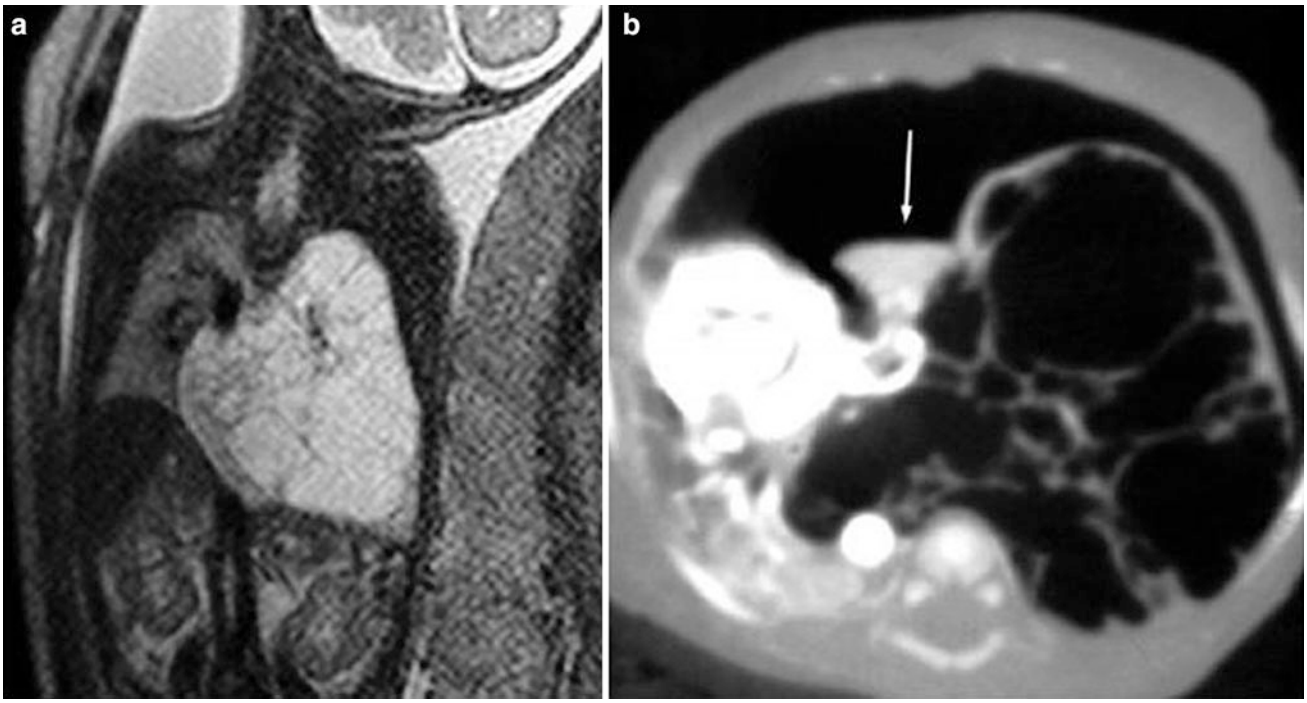

Fig. 8 CPAM type 1. **a** Coronal MR haste image in a 27-week-old fetus shows a large high signal intensity slightly heterogeneous mass with multiple septi arising from the left lung and crossing the midline. **b** A CT done when the patient was 5-day-old shows an anterior pneumothorax and multiple cysts occupying the left hemithorax, crossing the midline, displacing the heart to the right. A small collapsed superior lobe is seen (*arrow*)

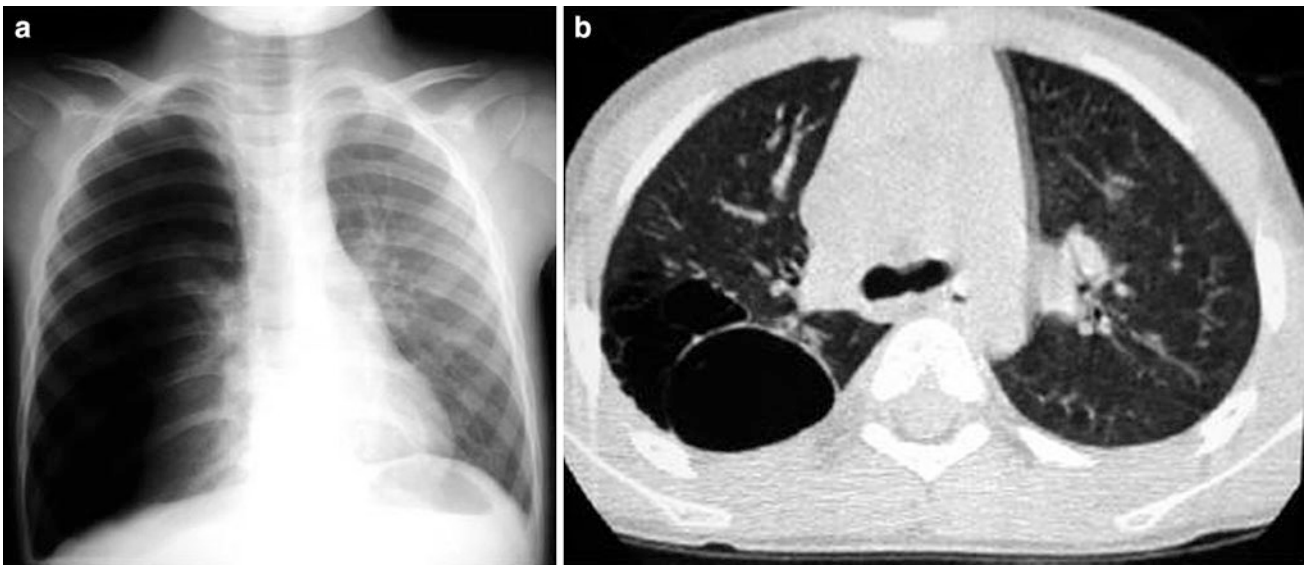

Fig. 9 Congenital pulmonary airway malformation type I in a 6-year-old girl with chest pain and dyspnea. **a** Chest radiograph shows right-sided pneumothorax. A chest tube was inserted and the lung was re-expanded. **b** Chest CT performed 1 week later reveals multiple cysts at the right upper lobe

preexisting cystic lung disease, but is reasonable to assume that the cystic changes are a component of the PPB, itself (Murphy et al. 1992). As the initial manifestation, pneumothorax is more frequently seen in PPB than in CPAM (Fig. 9) (Senac et al. 1991). However, pneumothorax can be found associated with both entities and the available information does not support the use of this finding as a differentiating diagnostic criteria (Lejeune et al. 1999).

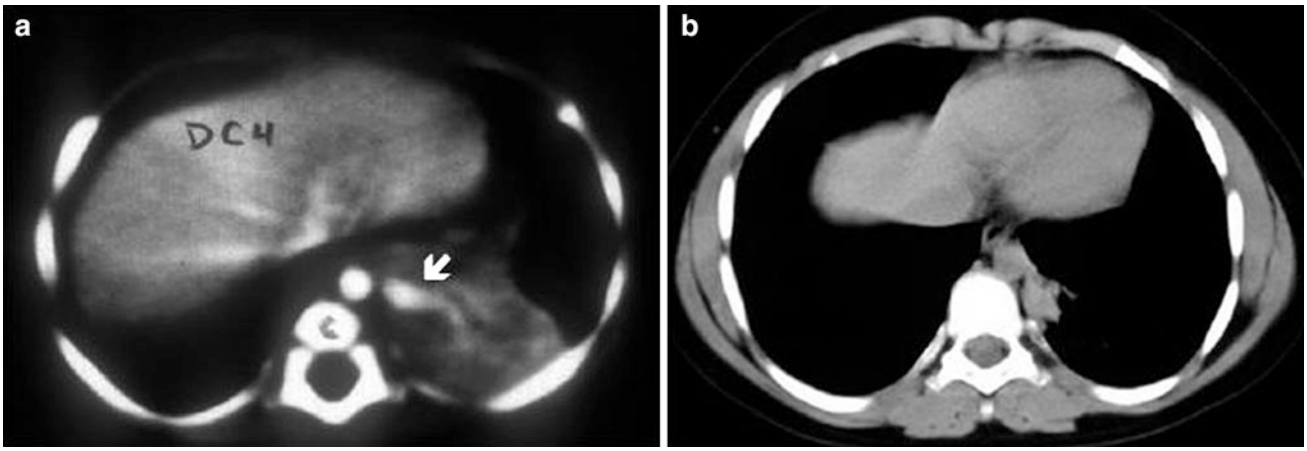

Fig. 10 Spontaneous involution of a pulmonary sequestration. **a** Contrast-enhanced chest CT at the age of 3 months shows a soft tissue density mass with a large feeding vessel originating from the aorta (*arrow*). **b** Significant shrinkage of the mass is seen in the scan at the age of 10 years

Cases of CPAM/pulmonary sequestration that dramatically decreased in size or disappear completely during pregnancy and infancy have been reported (Fig. 10). However, the clinical management of an asymptomatic child with a congenital mass of the lung remains controversial. Some authors advocate close clinical observation and radiological surveillance (MacGillivray et al. 1993), whereas others, considering the possibility that cystic pulmonary lesions may be infected (Garcia-Peña et al. 2013), or may be harbor or develop PPB, favor elective surgical resection (Samuel and Burge 1999).

2.3.2 Pulmonary Sequestration

Pulmonary sequestration consists of a mass of pulmonary tissue disconnected from the bronchial tree that receives its blood supply from the systemic circulation (Heitzman 1984). Pulmonary sequestration is divided into two groups: intralobar sequestration, in which the tissue is surrounded by normal lung and found in the interior of the visceral pleura, and extralobar sequestration, in which the tissue is disconnected from the bronchial tree and has its own pleural coating. In 1946 Pryce identified intralobar sequestration as a clinical-pathological entity. He was the first to apply the term "sequestration" and further classified the lesion as intralobar or extralobar on the basis of the morphologic patterns of the malformation. There are also mixed cases with characteristics of both intralobar and extralobar sequestration.

Pulmonary sequestration is an uncommon anomaly; the intralobar form is more frequent than the extralobar. Intralobar sequestration constitutes 75 % of all pulmonary sequestrations and is located in the left lower lobe in 60 % of the cases. Only 2 % occur in the upper lobes and 0.25 % in the middle lobe. The affected lung can maintain the normal lung architecture, behave like a mass, or present as internal cysts. Vascularization in the majority of cases is through the thoracic aorta (Savic et al. 1979), or less commonly, through systemic vessels originating from the abdominal aorta or one of its branches (Pedersen et al. 1988). The systemic supply can be formed by multiple, small-caliber blood vessels or by a single vessel, which are histologically similar to the pulmonary artery. This favors the early appearance of atherosclerosis (Ikezoe et al. 1990). Intralobar sequestration does not receive blood from the pulmonary arteries and it drains through pulmonary veins. In exceptional cases it communicates with the digestive tract (bronchopulmonary foregut malformation) (Hruban et al. 1989). It can be bilateral, or associated with other congenital malformations.

Since Pryce's description of pulmonary sequestration, there has been considerable controversy about its origin. Some authors contend that intralobar sequestration is, in fact, acquired (Gebauer and Mason 1959; Holder and Langston 1986), resulting from endobronchial obstruction leading to chronic pulmonary infection and hypertrophy of the systemic arteries in and around the area of the pulmonary ligament. This explains why, in the past, when infections were poorly controlled, intralobar sequestration was overdiagnosed. However, congenital intralobar sequestration does occur, since this anomaly has been recognized on prenatal US and has been detected in newborns (West et al. 1989; Laurin and Hägertrand 1999) (Fig. 11).

Intralobar sequestration is usually discovered because the patient has developed a pulmonary infection, although some patients are asymptomatic when the lesion is found. In a small number of cases intralobar sequestration debuts as a pulmonary hemorrhage (Fig. 12), pleural effusion (Kim et al. 1997; Lucaya et al. 1984), or pleural bleeding secondary to infarction of the sequestrated lung (Zumbro et al. 1974). On plain films, intralobar sequestration appears as a homogenous opacity mostly in the lower lobes. This opacity can simulate a mass with a well-defined border, or show

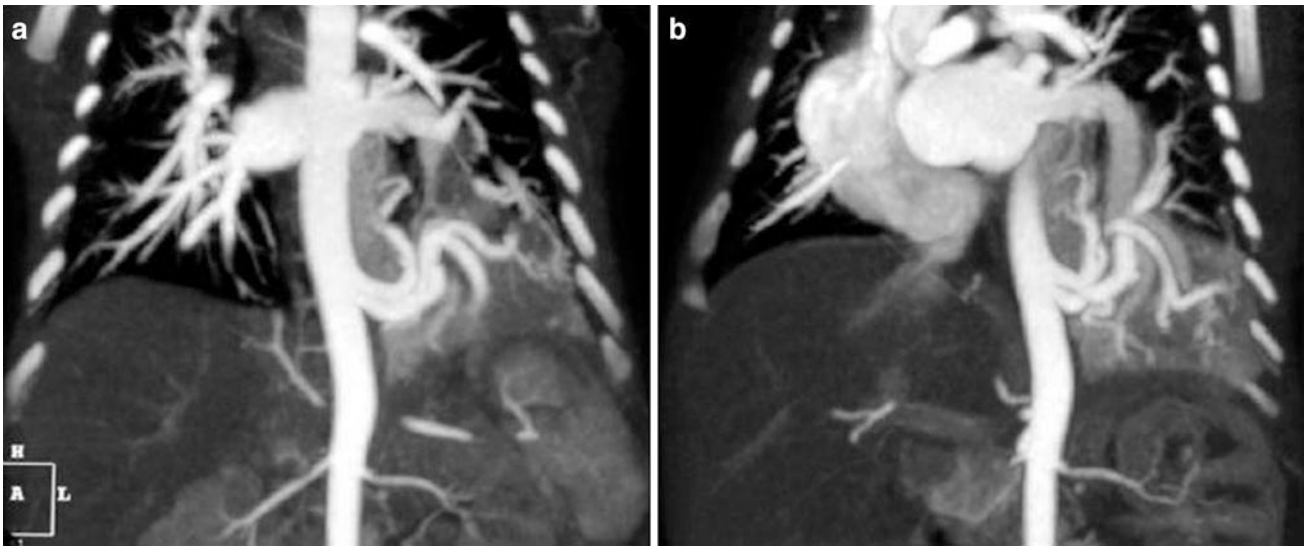

Fig. 11 Intralobar pulmonary sequestration in a 10-day-old boy with an echogenic mass in the left lower lobe seen on prenatal US. **a** Coronal MIP CT reconstructed image shows two anomalous arteries arising from thoracic aorta. **b** The drainage is through the lower left pulmonary vein

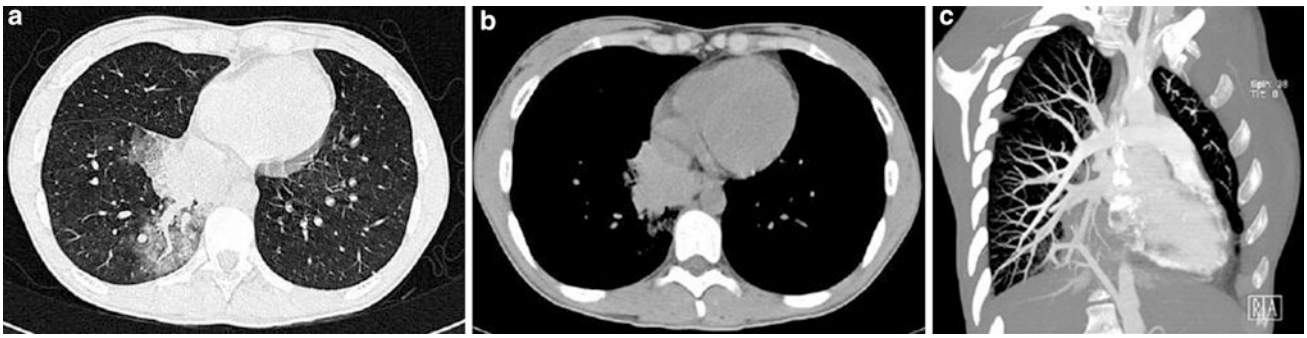

Fig. 12 Pulmonary sequestration in a 18-year-old with hemoptysis. **a** CT demonstrates the presence of ground glass area due to hemorrhage in the right lower lobe with a central vessel. **b** Shows a hyperdense mass secondary to hemorrhage into sequestration. **c** Angio-CT with MIP reconstructions shows that the vessel originates from the abdominal aorta

internal air–fluid levels and a poorly defined border. In rare cases calcifications are present within the sequestration or in the systemic blood vessel. An unusual presentation of intralobar sequestration is localized emphysema without an associated opacity or mass (Ko et al. 2000).

Extralobar sequestration is usually located between the lower lobe and the diaphragm, more frequently at the left thoracic base, in 77 % of cases (Savic et al. 1979). To a much lesser degree it has also been found in the mediastinum, pericardium (Stocker and Kagan-Hallet 1979), diaphragm, or retroperitoneum (Baker et al. 1982). Vascular supply occurs through a systemic artery and venous drainage through the azygos or portal system (Rees 1981), although nearly 25 % are completely or partially drained by pulmonary veins. Extralobar sequestration is associated with other congenital malformations in 65 % of cases, such as diaphragmatic hernia, bronchogenic cyst, BA, scimitar syndrome, pericardial defect and as previously stated, CCAM (Savic et al. 1979), and these are much more frequent than those associated with the intralobar form. Both types of sequestration occasionally can connect with the digestive tract (bronchopulmonary foregut malformation) (Hruban et al. 1989). The presence of air bronchograms within a mass thought to be ELS should suggest the diagnosis of bronchopulmonary foregut malformation. Communication between the tracheobronchial tree and the GI should be examined by upper GI series or MDCT. Extralobar sequestration is usually detected fortuitously and can also be associated with pleural effusion. It may be seen as a homogeneous mass or a small bump on the posterior hemidiaphragm that may be subtle and occasionally inapparent on the chest radiograph.

Ultrasound, CT, and MRI are useful in the study of sequestrations (Fig. 13). Multidetector CT angiography is considered the imaging technique of choice for preoperative evaluation of pulmonary sequestration. MDCT with

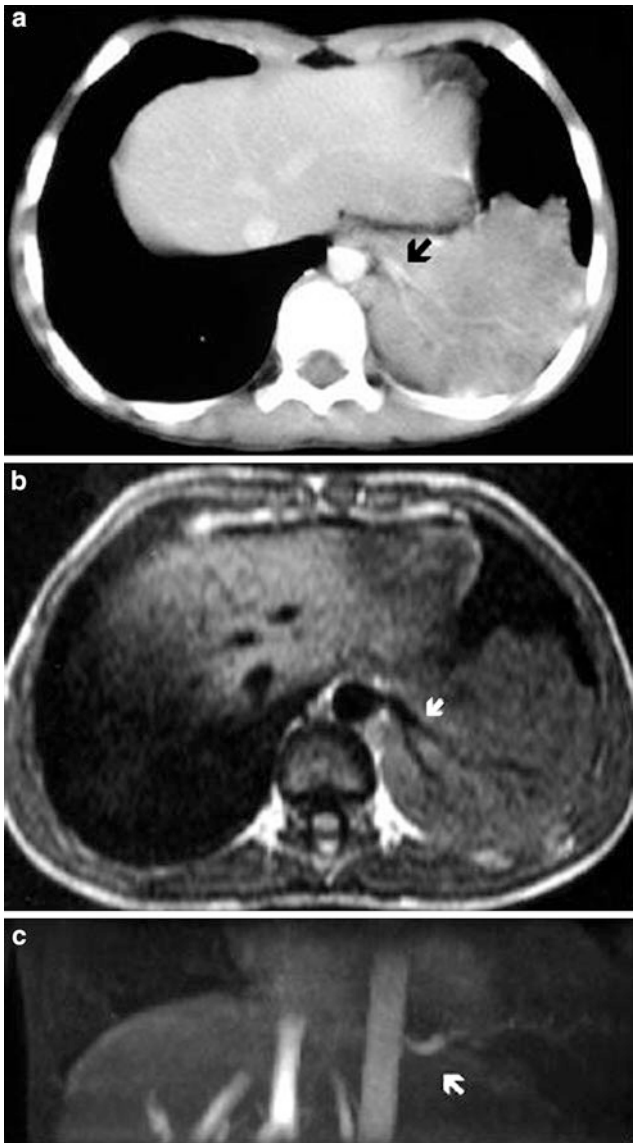

Fig. 13 Intralobar pulmonary sequestration of the left lower lobe in a 2-year-old boy. **a** Contrast-enhanced chest CT shows the sequestration and a systemic branching vessel originating from the aorta (*arrow*). **b** Axial SE T1-weighted and **c** coronal 2D TOF MIP reconstruction images demonstrate a branching feeding vessel originating from the descending aorta and supplying the pulmonary sequestration (*arrows*)

supplementary multiplanar and 3D images has the advantage of being able to show the pulmonary parenchyma abnormality, as well as the arterial and venous angioarchitecture of the sequestration (Lee et al. 2004, 2011a). CT has some advantages over MR angiography for evaluating pulmonary sequestrations in children. CT scan times are significantly shorter, and resolution of small vessels and lung parenchyma is better. CT in a single phase of contrast injection is adequate for evaluation of both the arterial and the venous anatomy, using low dose to minimize radiation (Abbey et al. 2009; Lee et al. 2011b). Intralobar sequestration typically manifests as a homogeneous or

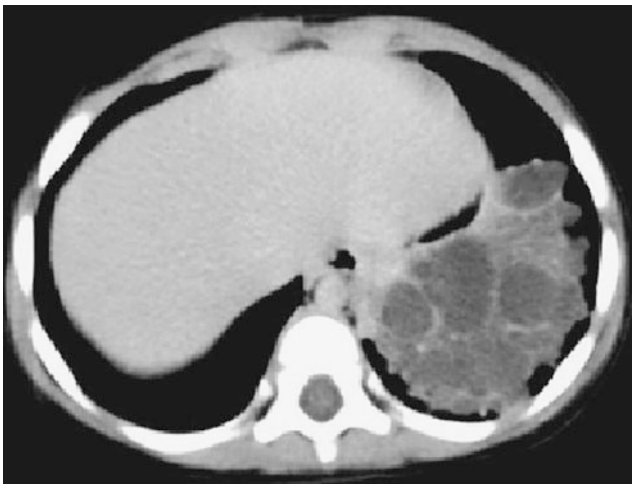

Fig. 14 Intralobar pulmonary sequestration in a 2-year-old boy. CT scan shows a mass with multiple fluid-filled cysts in the left lower lobe

inhomogeneous solid mass, with or without definable cystic changes. It can also appear as an aggregate of multiple small cystic lesions with air or fluid content (Fig. 14), a well-defined cystic mass, or a large cavitary lesion with air–fluid level. The lesion may enhance with contrast material (Frazier et al. 1997; Rosado-De-Christenson et al. 1993). An appearance simulating emphysema, possibly resulting from collateral ventilation and air-trapping, can sometimes be seen in sequestration. Expiratory CT scans are helpful for delineating the extent of the malformation (Fig. 15) (Stern et al. 2000; Lucaya et al. 2000). Extralobar sequestration is seen on chest CT as a homogeneous, well-delimited mass, sometimes with internal cystic areas (Rosado-De-Christenson et al. 1993).

MR imaging is a safe and noninvasive imaging method, which may be useful in some specific cases of pulmonary sequestration (Naidich et al. 1988; Yu et al. 2010). In MR, this anomaly is seen as a well-defined, irregular, or branch-like mass. MR can also reveal the presence of cystic areas, as well as the variable solid, fluid, hemorrhagic, and mucus-containing components. However, MR imaging cannot delineate focal thin-walled cysts or the emphysematous changes of sequestration as clearly as CT. The size, origin, and course of the aberrant systemic artery and the venous drainage can be demonstrated by MR imaging. Breath-hold (if possible) or nonbreath-hold three-dimensional contrast-enhanced MR angiography offer excellent display of the aberrant vessel without flow artifacts (Ko et al. 2000). The advantage of MRI over CT is the absence of radiation. However, long scan times, sedation requirements, and suboptimal evaluation of lung parenchyma are the disadvantages of this method.

Nowadays, there is no place for conventional angiography in the diagnosis of pulmonary sequestration. Vascular

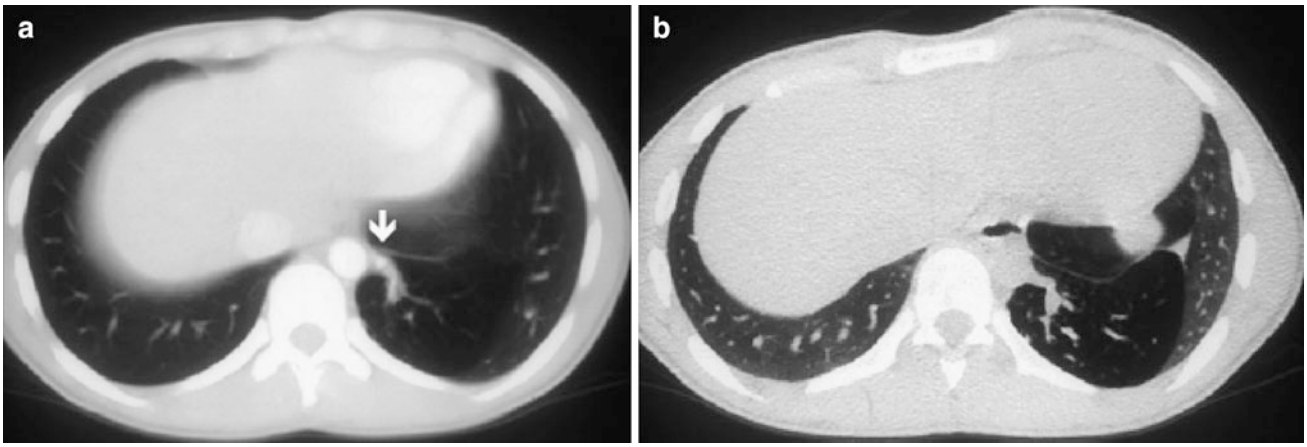

Fig. 15 Intralobar pulmonary sequestration in left lower lobe in a 15-year-old boy. **a** Enhanced CT scan shows hyperlucency in left lower lobe. A systemic vessel (*arrow*) originating from the aorta and feeding the sequestration is well defined. **b** In an expiratory high-resolution CT scan at same level as (**a**), air-trapping can be seen within the sequestered lung. (Reprinted with permission)

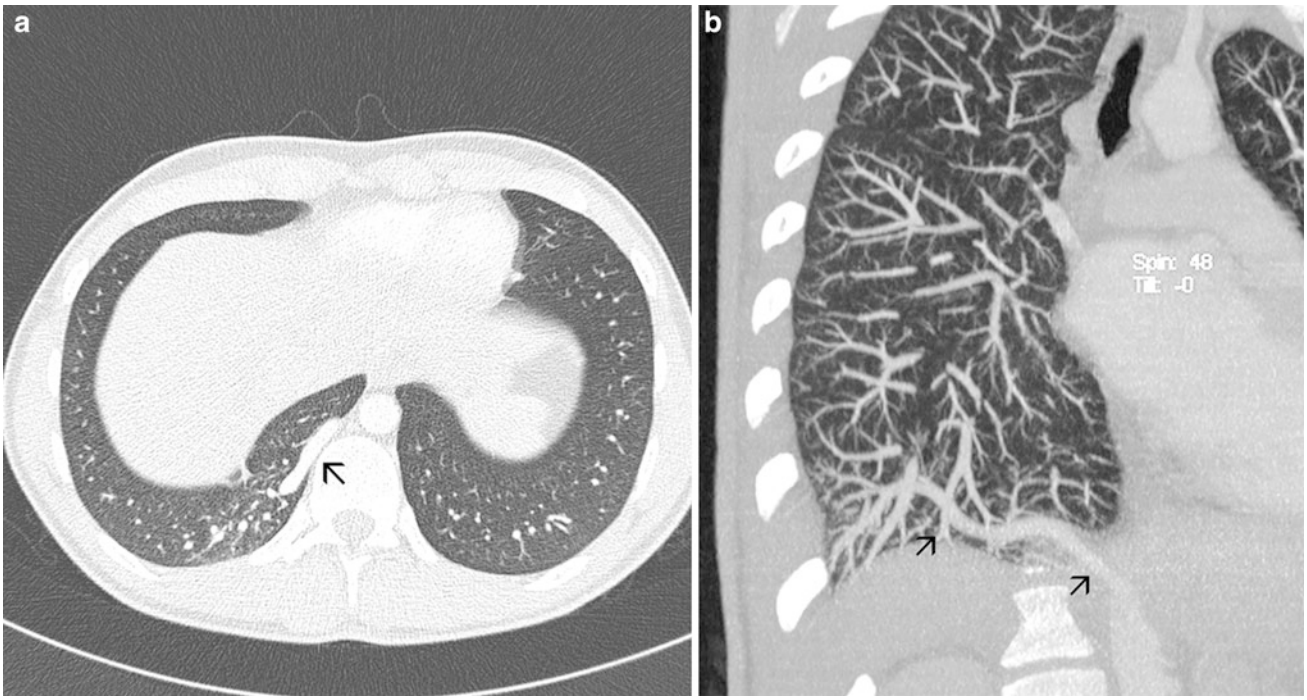

Fig. 16 Isolated systemic supply to normal lung in a 18-year-old. CT scan in **a** shows the anomalous vessel as a large tubular structure in the right lower lobe (*arrow*). The vessels in the tissue supplied by the systemic artery are larger than the remaining pulmonary artery vessels. CT angiogram with MIP reconstruction **b** shows the course of the anomalous systemic vessel from the abdominal aorta (*arrows*)

studies should be limited to cases in which embolization of feeding vessels is contemplated.

The treatment of bronchopulmonary sequestration (BPS) is controversial. Some authors consider that even in asymptomatic patients, BPS should be resected (Cho et al. 2012). Others consider endovascular treatment with selective embolization of the inflow arteries an attractive and minimally invasive therapeutic option (Marine et al. 2011). Nevertheless, other authors recommend nonsurgical management in asymptomatic patients due to the fact that BPS can decrease and even spontaneously disappear (see Fig. 10) (Garcia-Peña et al. 1998, 2013).

2.4 Isolated Systemic Supply to Normal Lung

Isolated systemic supply to normal lung is a variant of pulmonary sequestration. This malformation corresponds to type I of Pryce's classification (Pryce et al. 1947). The artery is typically large and supplies the normal lung

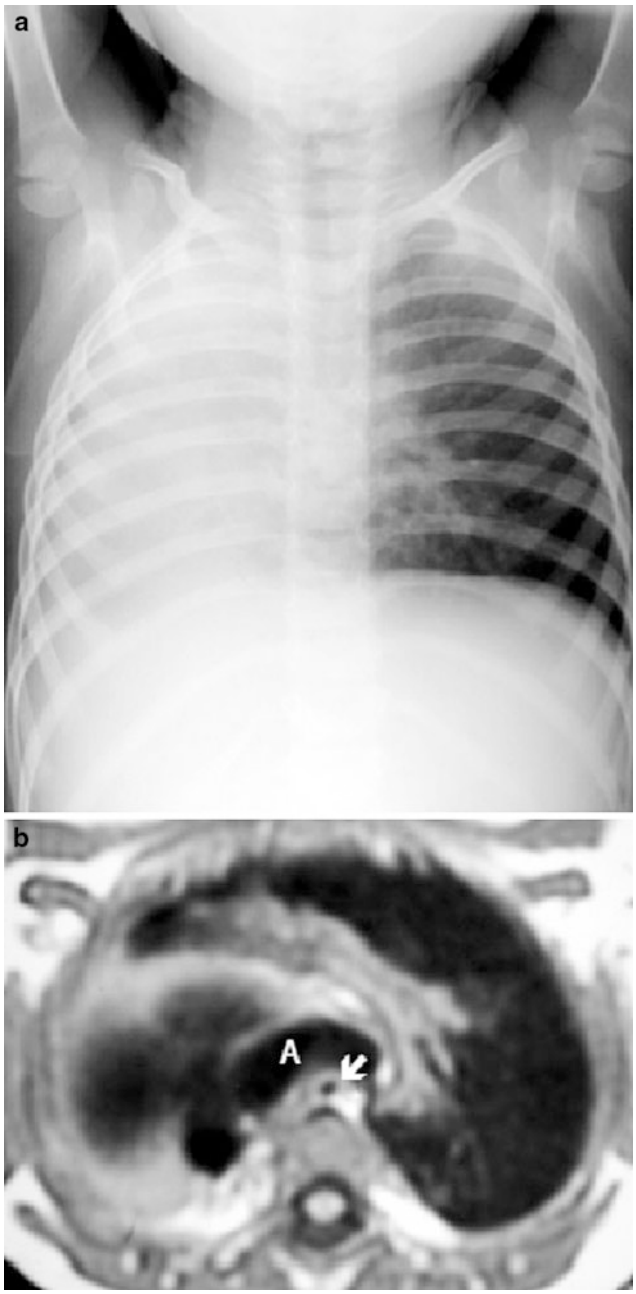

Fig. 17 Right lung aplasia in a 2-year-old boy with respiratory symptoms. **a** Chest radiograph shows opaque right hemithorax with cardiomediastinal displacement and left lung hyperinflation. **b** Axial MR image at the level of the aortic arch demonstrates severe narrowing and posterior displacement of the distal trachea (*arrow*) by the crossing arch (*A*)

connected to the bronchial tree; the lung bases are affected more often (Mäkinen et al. 1981). Patients are usually asymptomatic, although there may be a continuous murmur on the thoracic wall or heart failure secondary to left-to-left shunt. Associated hemoptysis occurs occasionally.

Chest radiographs show increased opacity due to the systemic artery. Sometimes well-defined tubular or rounded images produced by the anomalous vessels can be recognized. The pulmonary parenchyma does not present any other changes, unless there is associated hemorrhage. Definitive diagnosis can be established with MDCT identification of a systemic artery originating in the thoracic or abdominal aorta and absence of pathology of the underlying lung (Fig. 16) (Mata et al. 1991; Jiang et al. 2011).

3 Dysmorphic Lung

Dysmorphic lung (DL) is characterized by arrested development of either a whole lung (lung agenesis–hypoplasia complex) or a lobe (lobar agenesis–aplasia complex). Absence of a lobe may be associated with other abnormalities, some of them common and others highly unusual. DL can be recognized on chest radiographs when we are aware of its existence and it is sometimes possible to reach a diagnosis based solely on plain film evidence. In doubtful cases it is advisable to use CT (Mata et al. 1990; Woodring et al. 1994), or MRI (Baxter et al. 1990) to confirm the diagnosis.

3.1 Lung Agenesis–Hypoplasia Complex

Arrested development of a whole lung (lung agenesis–hypoplasia complex) is uncommon and occurs equally often in either hemithorax. Although the terms agenesis (absence of bronchus and lung), aplasia (absence of lung with bronchus present), and hypoplasia (bronchus and rudimentary lung present) describe different anomalies (Boyden 1955), we group all three under the term "agenesis–hypoplasia complex" because all have a similar radiologic appearance on the chest radiograph. In pediatric patients the prognosis for right-sided agenesis is worse than for left-sided lesions, due to a greater shift of the heart and mediastinum, resulting in a greater distortion of the airway and great vessels. Respiratory distress and recurrent infections are common in children with right-lung agenesis. Airway compression by vascular structures, such as the aortic arch, pulmonary artery and patent ductus arteriosus, as well as intrinsic tracheobronchial anomalies and tracheobronchomalacia have been described in patients with right-lung agenesis (Newman and Gondor 1997) (Fig. 17). A similar appearance has been reported in patients with the so-called right post-pneumonectomy syndrome.

Lung agenesis–hypoplasia complex can be associated with malformations in other systems, including the skeletal, digestive, cardiac and urinary systems, and even in the contralateral lung (Brünner and Nissen 1963). The incidence of lung agenesis–hypoplasia with malformations in the skeleton or other organs is very high in some series

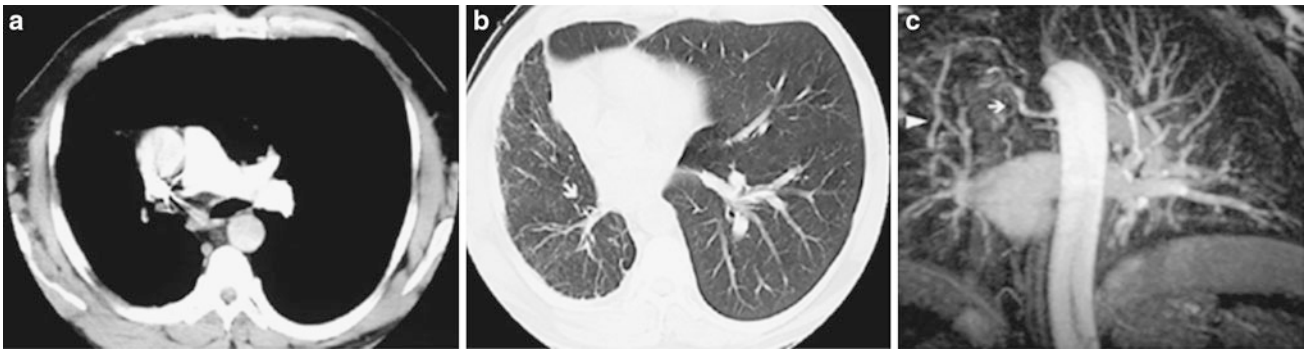

Fig. 18 Absence of proximal right pulmonary artery. **a** Contrast-enhanced CT scan reveals absence of the right pulmonary artery. **b** Axial CT image at lung window shows volume loss on right side with shift of heart and mediastinum and a tiny pulmonary vein (*arrow*). **c** Breath-hold coronal 3D GRE MIP reconstruction after dynamic gadolinium injection shows the presence of intercostal vessels (*arrowhead*) and bronchial arteries (*arrow*) arising from the aorta supplying the right lung

(Osborne et al. 1989). A common origin, such as insult to the neural crest in the embryo has been postulated to explain these phenomena, giving rise to the VACTERL syndrome of anomalies (Knowles et al. 1988).

Characteristically, lung agenesis–hypoplasia complex appears on the posteroanterior view as a diffuse opacity of one hemithorax with mediastinal shift, reminiscent of the appearance of whole lung atelectasis. Occasionally it presents an atypical appearance that is more difficult to recognize on plain film. The small hemithorax, aerated lung and apparent pleural thickening, simulate chronic pleural disease (Calenoff and Friederici 1964). This appearance results from the marked herniation of the contralateral lung. Typical and atypical cases show the same radiological appearance on the lateral chest view: retrosternal hyperclarity with the heart and large mediastinal vessels displaced backwards (Mata and Cáceres 1996).

CT demonstrates the reasons for the two distinct radiological presentations. Pulmonary herniation takes place behind the sternum in both groups and accounts for the retrosternal hyperclarity. Mediastinal rotation explains the posterior displacement of the heart and mediastinum. If the herniation of the contralateral lung is not severe, the plain film shows the typical appearance of a small opaque hemithorax. In atypical cases, the extensive herniation of the contralateral lung crosses the midline to penetrate deep into the malformed hemithorax, giving the appearance of aerated lung on plain films. The pseudo-thickening of the pleura is produced by accumulation of subpleural fatty tissue, filling the space left by the absent or underdeveloped lung (Mata et al. 1990). Lung agenesis, aplasia, and hypoplasia can be differentiated with use of CT, although the distinction is of little clinical significance. CT reveals the presence or absence of bronchi and pulmonary tissue, and allows measurement of the ipsilateral pulmonary artery (Mata and Cáceres 1996). Although lung agenesis–hypoplasia complex is said to go together with a small ipsilateral pulmonary artery, on CT or MRI studies a small number of patients show a near normal-sized pulmonary artery with substantial blood flow.

Absence (atresia or interruption) of the main right or left pulmonary artery (APA) is an isolated vascular malformation that goes together with small homolateral lung, but should not be considered a part of lung agenesis–hypoplasia complex. It usually occurs in association with cardiac anomalies; isolated APA is rare (Kleinman 1979). During childhood APA produces substantial bronchial and transpleural (intercostal arteries) collateral circulation. The enlarged bronchial and intercostal arteries that feed the lung sometimes produce hemoptysis. At radiologic study, APA is seen as a small lung with mediastinal shift and no identifiable pulmonary artery. Collateral systemic supply produces peripheral linear opacities and pleural thickening. CT and MRI show absence of the pulmonary artery and can identify the enlarged systemic arteries (Fig. 18).

3.2 Lobar Agenesis–Aplasia Complex

Lobar agenesis–aplasia complex is a group of pulmonary malformations affecting, almost exclusively, the right hemithorax. All of these malformations present pulmonary anomalies in the form of one or more absent or underdeveloped pulmonary lobe. Depending upon the associated venous malformation, we can look at this group as a continuum. At one extreme, the pulmonary malformation is isolated and the veins are normal (hypogenetic lung syndrome). The second step in the continuum includes the anomalous unilateral single pulmonary vein, which drains all the lung parenchyma into the left atrium (Hasuo et al. 1981). Next in line is the levo-atriocardinal vein; in this malformation there is an anomalous vein that drains the entire lung and connects the left atrium with a systemic vein

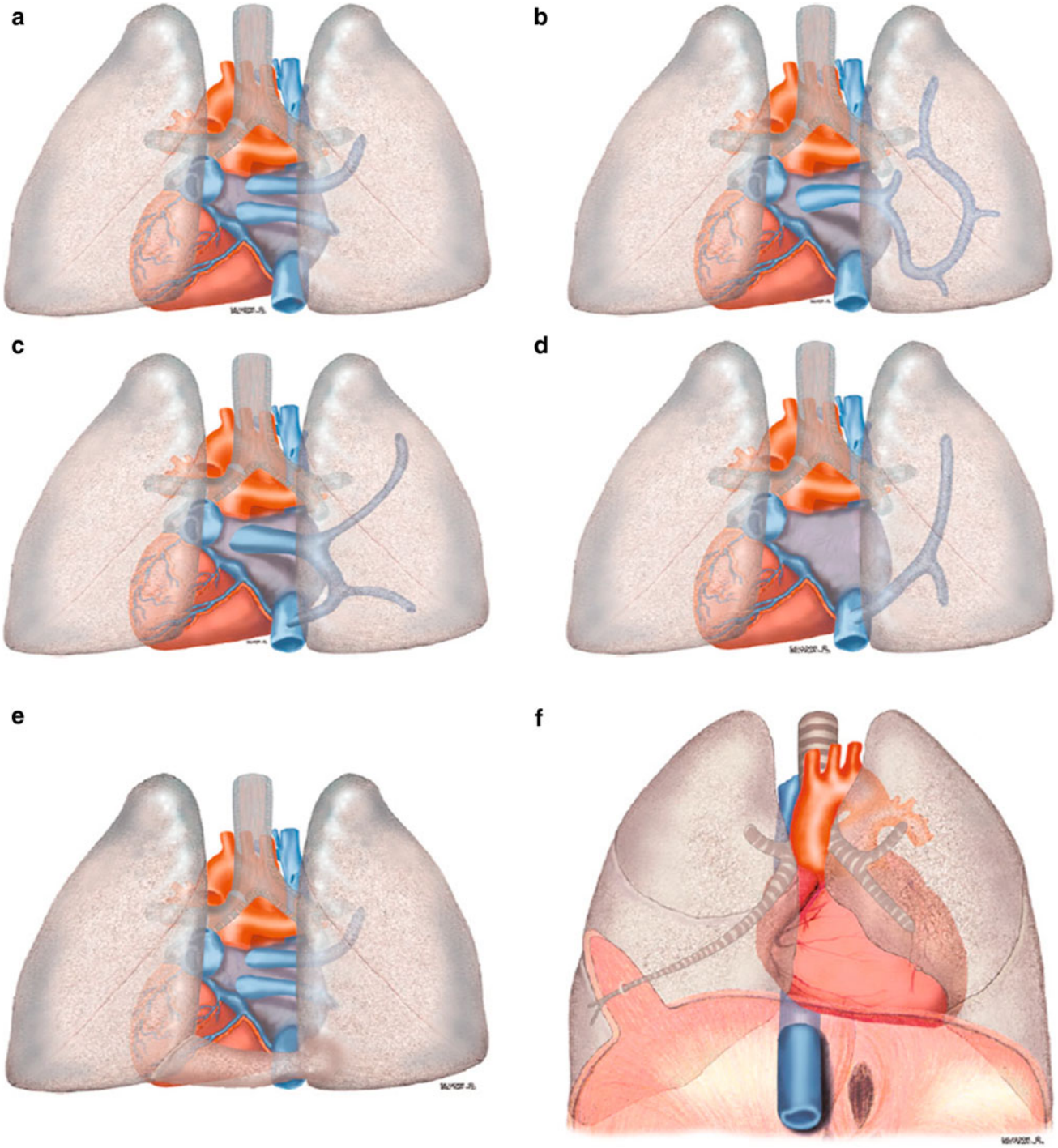

Fig. 19 The term lobar agenesis–aplasia comprises a complex group of pulmonary malformations with one or more absent or underdeveloped pulmonary lobes. Depending on the associated venous malformation, this group can be viewed as a continuum. At one extreme, the pulmonary malformation is isolated, and the veins are normal and drain into the left atrium (**a**). The second step of the continuum includes the anomalous unilateral single pulmonary vein, which drains the entire lung parenchyma into the left atrium (**b**). Next in line is the levo-atriocardinal vein, in which there is an anomalous vein that drains the entire lung and connects the left atrium with a systemic vein (inferior vena cava in the drawing) (**c**). Last in the continuum is an anomalous vein draining into the systemic venous system (venolobar syndrome) (**d**). Horseshoe lung (tissue from the malformed lung crossing the mediastinum to meet or fuse with the left lower lobe) (**e**) and accessory diaphragm (part of the right lung trapped by a membranomuscular duplication of the diaphragm) (**f**) can accompany any of these malformations

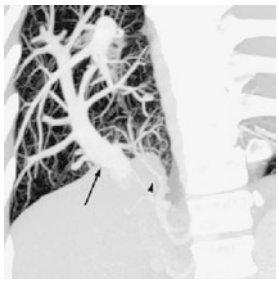

Fig. 20 Multiplanar reformation image. Congenital venolobar syndrome. We can see the scimitar vein (*arrow*) and the systemic supply from the abdominal aorta going to the right pulmonary base (*arrowheads*)

(Edwards and DuShane 1950). Last in the continuum is an anomalous vein draining into the systemic venous system (venolobar syndrome). Accessory diaphragm (part of the right lung trapped by a membranomuscular duplication of the diaphragm) (Nazarian et al. 1971) and horseshoe lung (tissue from the malformed lung crossing the mediastinum to meet or fuse with the left lower lobe) (Dische et al. 1974) can accompany any of these malformations (Fig. 19). Systemic supply from the thoracic aorta is almost always present, although it is hardly ever seen on plain film or CT scans (Fig. 20). Sometimes the systemic artery is thick, mimicking a scimitar vein (Partridge et al. 1988).

3.2.1 Hypogenetic Lung Syndrome

In hypogenetic lung syndrome there is agenesis or aplasia of one or two pulmonary lobes. Patients are usually asymptomatic. This entity almost always occurs in the right hemithorax; left hemithorax involvement is exceptional.

The chest radiograph shows a small right hemithorax with mediastinal shift to the right and haziness of the right cardiac border. In some cases, the right hilum is hidden by mediastinal rotation and cannot be seen, and in others the shape of the hilum is reminiscent of the left hilum. In most cases, lateral chest films show a retrosternal band caused by the interface between the shifted mediastinum and the anterior border of the underdeveloped lung (Ang and Proto 1984).

CT provides a wealth of information (Godwin and Tarver 1986; Mata and Cáceres 1996) by demonstrating the size of the pulmonary artery, the branching of the bronchi, and accompanying anomalies of the diaphragm (diaphragmatic hernias). If underdevelopment is very pronounced, one can observe extrapleural fat deposits along the thoracic wall simulating pleural thickening similar to, though not as striking as, those seen in the lung agenesis–hypoplasia complex (Mata et al. 1990). The right upper lobe is the most often affected. This gives a bronchial pattern of the right lung similar to that observed in the left lung in normal conditions (hypoarterial bronchus) (Fig. 21). CT demonstrates the pulmonary veins draining into their normal location, ruling out venous anomalies.

Fig. 21 Hypogenetic lung syndrome. CT scan shows left bronchial pattern in both lungs. The right lung is smaller than the left lung (Reprinted with permission)

3.2.2 Lobar Agenesis–Aplasia with Anomalous Unilateral Single Pulmonary Vein

The second step in the continuum is a symptom-free malformation, first described by Benfield et al. in 1971. It has received several names since its description: pulmonary varix, meandering right pulmonary vein, or scimitar sign with normal pulmonary venous drainage. In our experience, in most cases this malformation consists of a hypogenetic lung with a single anomalous vein draining the entire lung parenchyma into the left atrium. The vein follows an unusual pathway before it meets the left atrium.

In the chest radiograph anomalous unilateral single pulmonary vein usually has the same appearance as hypogenetic lung syndrome, plus a tubular and serpiginous shadow due to the anomalous vein. In rare cases the anomalous vein mimics a scimitar vein (Herer et al. 1988). MDCT and MRI provide the right diagnosis, showing a serpiginous shadow running through the lung and ending in the left atrium (Mata and Cáceres 1996) (Fig. 22). In some cases of anomalous unilateral single pulmonary vein, the vein drains into an extracardiac chamber located behind the left atrium (cor triatriatum).

Exceptionally we can see atypical cases with anomalous pulmonary veins affecting both lungs. This has been described as idiopathic prominence of pulmonary veins or "meandering pulmonary veins" (Kriss et al. 1995; Mata et al. 2000). The veins of both lungs follow an unusual pathway and drain into the left atrium. Meandering pulmonary veins is occasionally associated with hypogenetic lung.

Fig. 22 Anomalous right unilateral single pulmonary vein. Axial SE T1-weighted images at two different levels (**a**, **b**) reveal an enlarged and serpiginous right pulmonary vein (*arrows*) draining at the left atrium. **c** Coronal MR GRE 2D demonstrates the huge and tortuous single right pulmonary vein (*arrow*)

Fig. 23 Multiplanar reformation image showing a levo-atriocardinal vein (*arrow*) connecting an anomalous vein draining into the inferior cava vein and a pulmonary vein draining into the left atrium (Courtesy of José Cáceres M.D.)

3.2.3 Lobar Agenesis-Aplasia with Levo-atriocardinal Vein

Levo-atriocardinal vein is defined as an anomalous vein that connects the left atrium and one vein of the systemic venous system. The systemic venous system derives from the embryological system known as cardinal veins. The malformation consists of a hypogenetic lung with the anomalous vein connecting the left atrium and one of the main systemic veins. Levo-atriocardinal vein would be the midpoint in the continuum between anomalous unilateral single pulmonary vein and venolobar syndrome. It is a very uncommon malformation.

On chest radiography the levo-atriocardinal vein looks very similar to the anomalous unilateral single pulmonary vein. CT demonstrates the usual findings of hypogenetic lung syndrome and the vein joining the left atrium and a systemic vein (Fig. 23). The anomalous vein drains all the pulmonary veins, and MRI shows the pathway of the vein as well as the points where it meets with the systemic vein and the left atrium (Fig. 24) (Mata et al. 2000). MRI can demonstrate that there is no gradient between the left atrium and the systemic vein.

3.2.4 Congenital Venolobar Syndrome

In congenital venolobar syndrome (CVS), also known as scimitar syndrome, partial anomalous venous return (PAVR) is associated with hypogenetic lung syndrome. This malformation is one of the extremes of the DL continuum. Other components of the syndrome are an absent or small right pulmonary artery, anomalous systemic arterial supply of the lung from the thoracic or abdominal aorta, absence of the inferior vena cava, and anomalies of the hemidiaphragm (hernia, eventration, partial absence, accessory diaphragm). Bronchial tree anomalies (abnormal distribution, stenosis), esophageal and gastric lung (communication between sequestered lung and the esophagus or stomach), horseshoe lung, anomalous superior vena cava, and absence of the left pericardium are less frequently seen.

Congenital heart disease, most commonly atrial septal defects, is present in approximately 25 % of patients. Ventricular septal defects, patent ductus, tetralogy of Fallot, endocardial cushion defects, and aortic coarctation have also been reported.

Most adults and older children are asymptomatic. The left–right shunt produced by the anomalous drainage is usually small and has no clinical repercussions, though on rare occasions it can lead to pulmonary hypertension (Haworth et al. 1983). When scimitar syndrome presents during infancy, symptoms are usually severe and there are complex associated anomalies such as cardiac defects and anomalous systemic supply to the lung. (Canter et al. 1986). CVS occurs almost exclusively in the right hemithorax.

Fig. 24 Levo-atriocardinal vein in the right lung. Axial MR GRE 2D images at three different levels (**a**–**c**) show the tortuous vein that goes from the left atrium to the inferior vena cava (*arrows*)

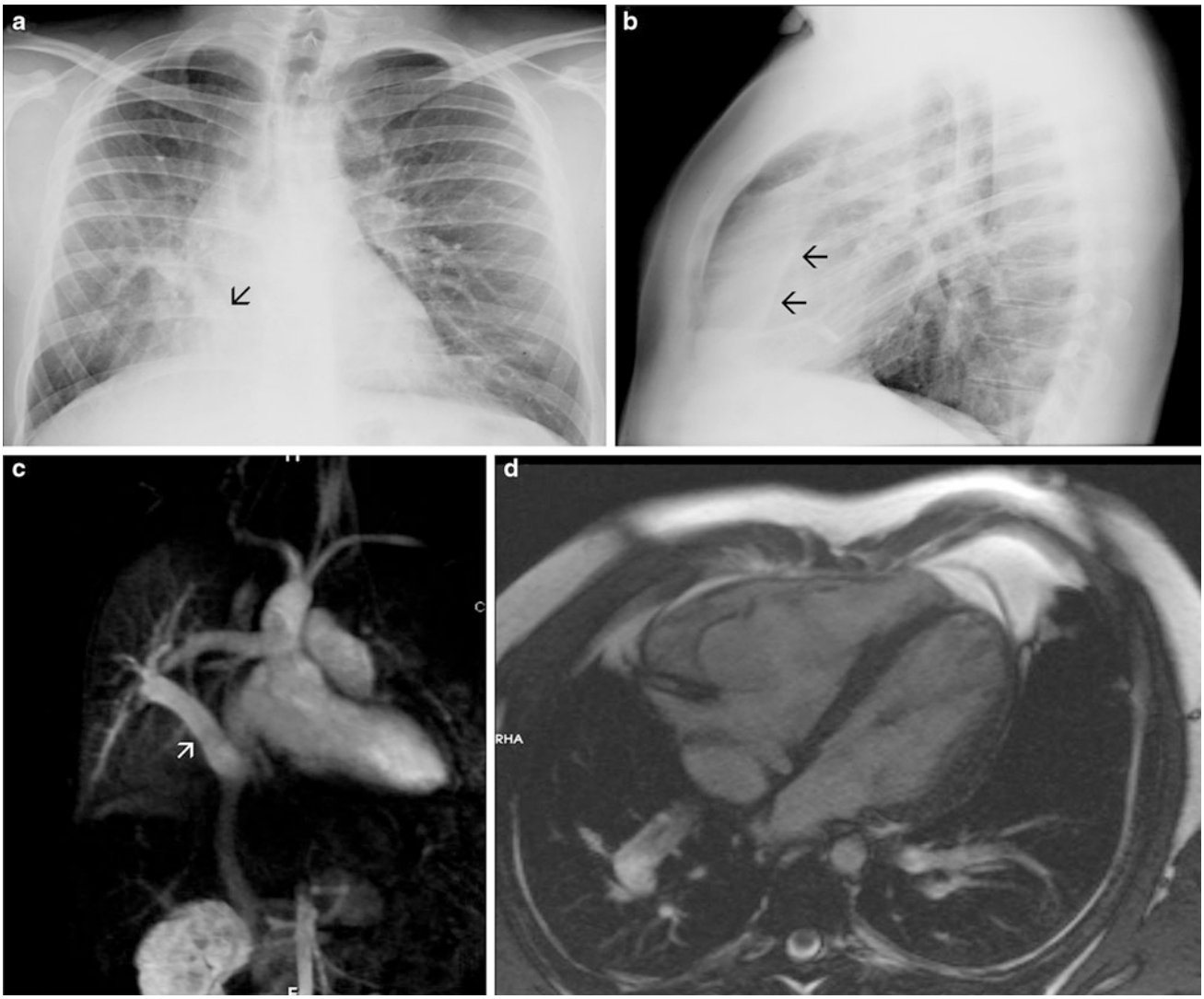

Fig. 25 Venolobar syndrome **a** Chest plain film shows a tubular image in the right pulmonary base (*arrow*) and an elevation of right diaphragm secondary to diaphragmatic eventration; the right lung is smaller than the left lung. The lateral view **b** shows a retrosternal band (*arrows*) **c** MR angiogram reveals the scimitar vein (*arrow*) draining to the suprahepatic portion of the inferior vena cava. **d** Bright-blood MR image shows right ventricular dilatation

Plain film findings are similar to those of hypogenetic lung. The differential finding is the anomalous vein. The vessel is seen as a widening tubular shadow that extends toward the base of the lung, originating the term scimitar syndrome. The anomalous vein usually drains into the inferior vena cava or the right atrium. Less commonly,

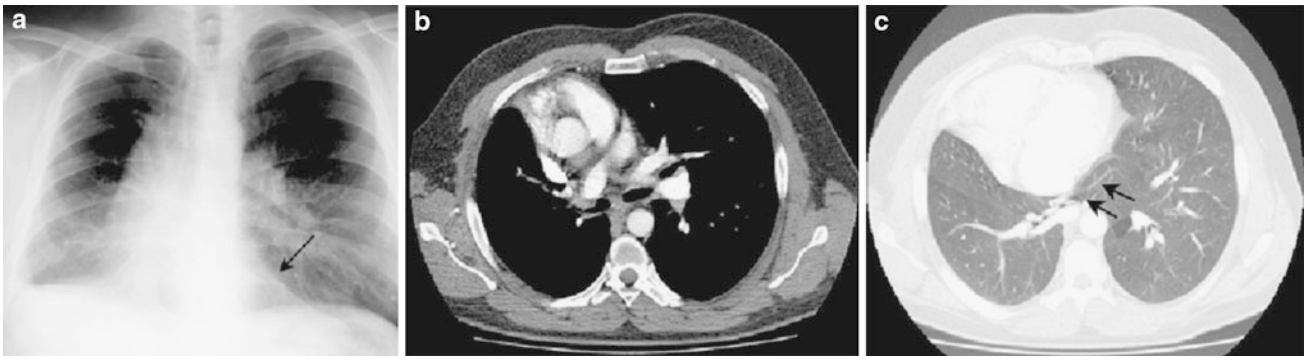

Fig. 26 Horseshoe lung. Plain film **a** shows a small right hemithorax and a linear image in the left pulmonary base (*arrow*). CT demonstrates the anomalous pattern of right bronchial tree and the mediastinal shift (**b**). In **c** we can see the mediastinal discontinuity behind the heart and right lower lobe arteries and bronchus (*arrows*) crossing the midline, going to the left pulmonary base

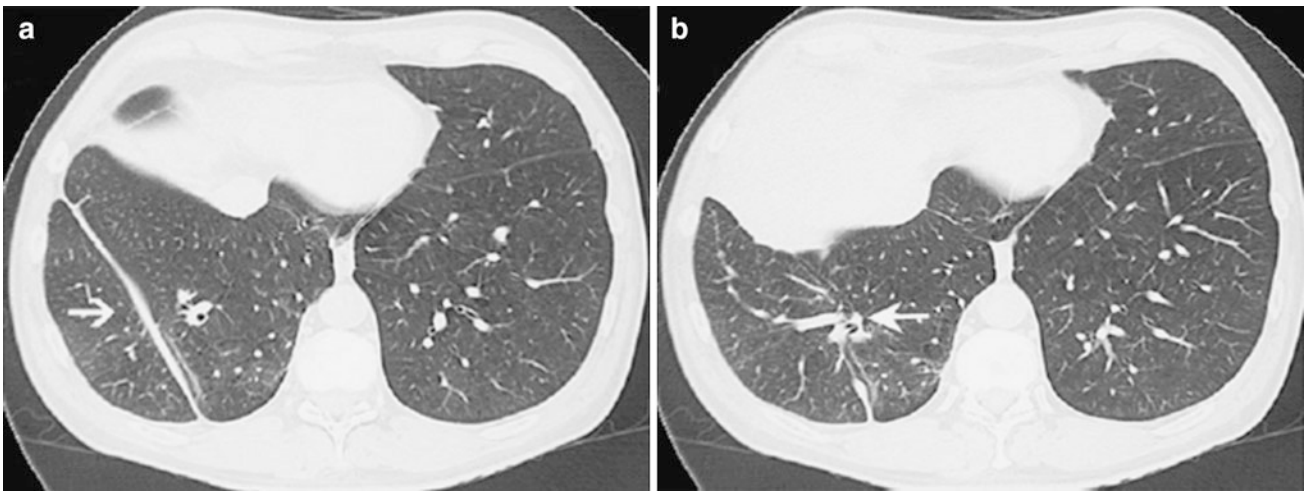

Fig. 27 Accessory diaphragm. **a** The accessory diaphragm can be seen by CT as a line, simulating a fissure (*arrow*). **b** The vessels and bronchus are crowded together as they go through the central hole (*arrow*)

PAVR drains into the hepatic or portal veins, azygos system or coronary sinus. This drainage can be stenotic at its implantation. The fact there may be more than one vein or that a single vein may be hidden behind the displaced heart, accounts for the fact that the PAVR is not seen on plain films in half the cases.

Contrast-enhanced MDCT and gadolinium-enhanced MR angiography will show the anomalous pulmonary venous return, its course and drainage, the pulmonary artery, the systemic circulation to the lung (Mata et al. 1990; Woodring et al. 1994; Castellote et al. 2005) (Fig. 25), and the absence of pulmonary veins. PAVR is associated with an accessory pulmonary fissure that is visible on CT study (Godwin and Tarver 1986). MDCT scan may add information about bronchial anatomy and tracheobronchial abnormalities, septal lines (when the anomalous pulmonary return is obstructed), horseshoe lung, and other diaphragm malformations. Nevertheless, MR imaging provides functional data such as ventricular volumetry, ventricular function, flow analysis, and flow quantification, which may be used to calculate the left-to-right shunt fraction. These functional data enable the cardiologist to determine the functional importance of the lesion.

Surgery is reserved for patients with severe symptoms, usually due to a substantial left-to-right shunt with right ventricular dilatation (from volume overload) (Vyas et al. 2012).

3.2.5 Horseshoe Lung

Horseshoe lung is associated with hypogenetic lung syndrome and occurs when a small quantity of right pulmonary tissue arising from the lower lobe crosses the midline and joins the left lower lung. The right and left lower lobes may fuse, or be separated by a fissure. The isthmus of pulmonary tissue crosses the mediastinum behind the pericardium, in front of the aorta and the esophagus, and it is supplied by the right lower lobe vessels and bronchus (Frank et al. 1986; Freedom et al. 1986).

The chest radiograph shows hypogenetic lung syndrome or CVS together with an anomalous fissure in the base of the left lung. This finding suggests the correct diagnosis on the PA chest film (Frank et al. 1986). Sometimes the anomalous fissure can be seen as a thick opacity due to internal fat. CT shows the typical findings of hypogenetic lung, with or without abnormal veins, plus two additional findings: mediastinal discontinuity behind the heart, with the vessels of the right lower lobe crossing the midline and, when present, an anomalous fissure located at the base of the left lung (Fig. 26) (Beitzke et al. 1982).

3.2.6 Accessory Diaphragm

Accessory diaphragm, also known as diaphragmatic duplication, is a rare congenital anomaly associated with the lobar agenesis–aplasia complex. It does not occur as an isolated malformation. Accessory diaphragm was first described by Drake et al. in 1950. These authors postulated that the anomaly is produced in the initial stages of embryonic development when the septum transversum, which gives rise to the diaphragm, is in a very high position. If for some reason the descent of the septum transversum is arrested, part of the primitive lung can be trapped by it. The septum transversum would remain anchored to the posterior wall, creating an additional diaphragmatic leaf.

Accessory diaphragm is a thin fibromuscular membrane fused anteriorly with the diaphragm and coursing posterosuperiorly to join the posterior chest wall. It produces two compartments in the right hemithorax, trapping part of the lung parenchyma (Wille et al. 1975). The vessels and bronchi that supply the trapped lung pass through a central hole in the accessory diaphragm.

The accessory diaphragm can have two different appearances in the chest radiograph. When the central hiatus is very narrow, the trapped lung is not aerated and appears as a mass. When the trapped lung is aerated, the accessory diaphragm appears in plain film as a thin oblique line in either the posteroanterior or lateral chest view. In some patients a haziness is visible where the duplicated diaphragm joins the normal one.

When the lung is aerated, CT scans show the accessory diaphragm as a fissure-like line with a hole in the center (Woodring et al. 1994; Hidalgo et al. 2006) (Fig. 27). Depending upon the size of the central hole, the CT appearance varies. When the hole is large, it may be difficult to identify the accessory diaphragm. When the hole is small, the trapped lung may be opaque or hyperlucent, due to air-trapping. Vessels and bronchi are crowded together when they go through the central hiatus.

References

Abbey P, Das CJ, Pangtey GS, Seith A, Dutta R, Kumar A (2009) Imaging in bronchopulmonary sequestration. J Med Imaging Radiat Oncol 53:22–31

Ang JGP, Proto A (1984) CT demonstration of congenital pulmonary venolobar syndrome. J Comput Assist Tomogr 8:753–757

Baker EM (1989) Intrathoracic duplication cysts: a review of 17 patients. J Med Imaging 3:127–134

Baker EL, Gore RM, Moss AA (1982) Retroperitoneal pulmonary sequestration: computed tomographic findings. Am J Roentgenol 138:956–957

Bankoff MS, Daly BDT, Johnson HA, Carter BL (1985) Bronchogenic cyst causing superior vena cava obstruction: CT appearance. J Comput Assist Tomogr 9:951–952

Baxter R, McFadden PM, Gradman M, Wright A (1990) Scimitar syndrome: cine magnetic resonance imaging demonstration of anomalous pulmonary venous drainage. Ann Thorac Surg 50:121–123

Beitzke VA, Gypser G, Sager WD (1982) Scimitarsyndrom mit Hufeisenlunge. ROFO 136:265–269

Benfield JR, Gots RE, Mills D (1971) Anomalous single left pulmonary vein mimicking a parenchymal nodule. Chest 59:101–102

Biyyam DR, Chapman T, Ferguson MR, Deutsch G, Dighe MK (2010) Congenital lung abnormalities: embryologic features, prenatal diagnosis, and postnatal radiologic-pathologic correlation. Radiographics 30:1721–1738

Boyden EA (1955) Developmental anomalies of the lung. Am J Surg 89:79–89

Braffman B, Keller R, Stein Gendal E, Finkel SI (1988) Subdiaphragmatic bronchogenic cyst with gastric communication. Gastrointest Radiol 13:309–311

Brünner S, Nissen E (1963) Agenesis of the lung. Am Rev Respir Dis 78:103–106

Cachia R, Sobonya RE (1981) Congenital cystic adenomatoid malformation of the lung with bronchial atresia. Hum Pathol 12:947–950

Calenoff L, Friederici HH (1964) Unilateral pulmonary hypoplasia in an adult. Am J Roentgenol 91:265–272

Canter CE, Martin TC, Spray TL, Weldon CS, Strauss AW (1986) Scimitar syndrome in childhood. Am J Cardiol 58:652–654

Castellote A, Enriquez G, Lucaya J (2005) Congenital malformations of the chest beyond the neonatal period. In: Carty H, Brunelle F, Stringer DA, Kao SC-S (eds) Imaging children, Elsevier, Amsterdam

Ch'in KY, Tang MY (1949) Congenital adenomatoid malformation of one lobe of the lung with general anasarca. Arch Pathol 48:221–229

Cho MJ, Kim DY, Kim SC et al (2012) Embolization versus surgical resection of pulmonary sequestration: clinical experience with a thoracoscopic approach. J Pediatr Surg 12:2228–2233

Dische MR, Teixeira ML, Winchester PA, Engle MA (1974) Horseshoe lung associated with a variant of the "scimitar" syndrome. Br Heart J 36:617–620

Drake EH, Portland ME, Lynch JP (1950) Bronchiectasis associated with anomaly of the right pulmonary vein and right diaphragm. J Thorac Surg 19:433

DuMontier C, Graviss ER, Silberstein MJ, McAlister WH (1985) Bronchogenic cysts in children. Clin Radiol 36:431–436

Edwards JE, DuShane JW (1950) Thoracic venous anomalies. Arch Pathol 49:517
Felson B (1979) Mucoid impaction (inspissated secretions) in segmental bronchial obstruction. Radiology 133:9–16
Finck S, Milne ENC (1988) A case report of segmental atresia: Radiologic evaluation including computed tomography and magnetic resonance imaging. J Thorac Imag 3:53–57
Frank JL, Poole CA, Rosas G (1986) Horseshoe lung: clinical, pathologic, and radiologic features and a new plain film finding. Am J Roentgenol 146:217–226
Frazier AA, Rosado-de-Christenson M, Stocker JT, Templenton PA (1997) Intralobar sequestration: radiologic-pathologic correlation. Radiographics 17:725–745
Freedom RM, Burrows PE, Moes CAF (1986) "Horseshoe" lung: report of five new cases. Am J Roentgenol 146:211–215
Garcia-Peña P, Lucaya J, Hendry GMA et al (1998) Spontaneous involution of pulmonary sequestration in children: a report of two cases and review of the literature. Pediatr Radiol 28:266–270
Garcia-Peña P, Coma A, Enriquez G (2013) Congenital lung malformations: radiological findings and clues for differential diagnosis. Acta Radiol. doi:10.1177/0284185113475919
Gebauer PW, Mason CB (1959) Intralobar pulmonary sequestration associated with anomalous pulmonary vessels: a nonentity. Dis Chest 35:282–287
Godwin JD, Tarver RD (1986) Scimitar syndrome: four new cases examined with CT. Radiology 159:15–20
Grewal RG, Yip CK (1994) Intralobar pulmonary sequestration and mediastinal broncogenic cyst. Thorax 49:615–616
Griscom NT (1993) Diseases of the trachea, bronchi, and smaller airways. Radiol Clin North Am 31605–615
Hasuo K, Numaguchi Y, Kishikawa T, Ikeda J, Matsuura K (1981) Anomalous unilateral single pulmonary vein mimicking pulmonary varices. Chest 79:602–604
Haworth SG, Sauer U, Bühlmeyer K (1983) Pulmonary hypertension in scimitar syndrome in infancy. Br Heart J 50:182–189
Heitzman ER (1984) The lung: radiologic-pathologic correlations. Mosby, St Louis
Herer B, Jaubert F, Delaisements C, Huchon G, Chretien J (1988) Scimitar sign with normal pulmonary venous drainage and anomalous inferior vena cava. Thorax 43:651–652
Hidalgo A, Franquet T, Gimenez A (2006) 16-MDCT and MR angiography of accessory diaphragm. AJR 187:149–152
Holder PD, Langston C (1986) Intralobar pulmonary sequestration (a nonentity?). Pediatr Pulmonol 2:147–153
Hruban RH, Shumway SJ, Orel SB, Dumler JS, Baker RR, Hutchins M (1989) Congenital pulmonary foregut malformations. Intralobar and extralobar pulmonary sequestration communicating with the foregut. Am J Clin Pathol 91:403–408
Hugosson C, Rabeeah A, Al-Rawaf A et al (1995) Congenital bilobar emphysema. Pediatr Radiol 25:649–651
Ikezoe J, Murayama S, Godwin JD, Done SL, Verschakelenm JA (1990) Bronchopulmonary sequestration: CT assessment. Radiology 176:375–379
Jederlinic PJ, Sicilian LS, Baigelman W, Gaensler EA (1986) Congenital bronchial atresia. Medicine 65:73–83
Jiang S, Shi JY, Zhu XH et al (2011) Endovascular embolization of the complete type of anomalous systemic arterial supply to normal basal lung segments a report of four cases and literature review. Chest 139:1506–1513
Kim WS, Lee KS, Kim IO et al (1997) Congenital cystic adenomatoid malformation of the lung. CT-pathologic correlation. Am J Roentgenol 168:47–53
Kimura A, Makuuchi M, Takayasu K, Sakamoto M, Hiroshashi S (1990) Ciliated hepatic foregut cyst with solid tumor appearance on CT. J Comput Assist Tomogr 14:1016–1018
Kleinman PK (1979) Pleural telangiectasia and absence of a pulmonary artery. Radiology 132:281–284
Knowles S, Thomas RM, Lindenbaum RH, Keeling JW, Winter RM (1988) Pulmonary agenesis as part of the VACTERL sequence. Arch Dis Child 63:723–726
Ko SF, Ng SH, Lee TZ et al (2000) Noninvasive imaging of bronchopulmonary sequestration. Am J Roentgenol 175: 1005–1012
Kriss VM, Woodring JH, Cottrill CM (1995) "Meandering" pulmonary veins: report of a case in an asymptomatic 12-year-old girl. J Thorac Imaging 10:142–145
Kuhn C, Khun JP (1992) Coexistence of bronchial atresia and bronchogenic cyst: diagnostic criteria and embryologic considerations. Pediatr Radiol 22:568–570
Kwak GL, Stork WI, Greenberg SD (1971) Partial defect of the pericardium associated with a bronchogenic cyst. Radiology 101:287–288
Langston C (2003) New concepts in the pathology of congenital lung malformations. Semin Pediatr Surg 12:17–37
Laurin S, Hägertrand I (1999) Intralobar bronchopulmonary sequestration in the newborn—a congenital malformation. Pediatr Radiol 29:174–178
Lee EY, Siegel MJ, Sierra LM et al (2004) Evaluation of angioarchitecture of pulmonary sequestration in pediatric patients using 3D MDCT angiography. AJR Am J Roentgenol 183:183–188
Lee EY, Tracy DA, Mahmood SA et al (2011a) Preoperative MDCT evaluation of congenital lung anomalies in children: comparison of axial, multiplanar and 3 D images. Am J Roentgenol 196:1040–1046
Lee EY, Dorkin H, Vargas SO (2011b) Congenital pulmonary malformations in pediatric patients: review and update on etiology, classification, and imaging findings. Radiol Clin North Am 49:921–948
Lejeune C, Deschildre A, Thumerelle C et al (1999) Pneumothorax revealing cystic adenomatoid malformation of the lung in a 13 year old boy. Arch Pediatr 6:863–866
Lemire P, Trepanier A, Hebert G (1970) Bronchocele and blocked bronchiectasis. Am J Roentgenol 110:687–693
Lucaya J, García-Conesa JA, Bernadó L (1984) Pulmonary sequestration associated with unilateral pulmonary hypoplasia and massive pleural effusion. Pediatr Radiol 14:228–229
Lucaya J, García-Peña P, Herrera L et al (2000) Expiratory chest CT in children. Am J Roentgenol 174:235–241
Lyon RD, McAdams HP (1993) Mediastinal bronchogenic cyst demonstration of a fluid–fluid level at MR imaging. Radiology 186:427–428
MacGillivray TE, Harrison MR, Goldstein RB, Adzik SA (1993) Disappearing fetal lung lesions. J Pediatr Surg 28:1321–1325
MacSweeney F, Papagiannopoulos K, Goldstraw P (2003) An assessment of the expanded classification of congenital cystic adenomatoid malformations and their relationship to malignant transformation. Am J Surg Pathol 27(8):1139–1146
Mäkinen EO, Merikanto J, Rikalinen H, Satokari K (1981) Intralobar pulmonary sequestration occurring without alteration of pulmonary parenchyma. Pediatr Radiol 10:237–240
Marine LM, Valdes FE, Mertens RM et al (2011) Endovascular treatment pf symptomatic pulmonary sequestration. Ann Vasc Surg 25:696.e11-5
Martin KW, Siegel MJ, Chesna E (1988) Spontaneous resolution of mediastinal cysts. Am J Roentgenol 150:1131–1132
Mata JM, Cáceres J (1996) The dysmorphic lung: imaging findings. Eur Radiol 6:403–414
Mata JM, Cáceres J, Lucaya J, García-Conesa JA (1990) CT of congenital malformations of the lung. Radiographics 10:651–674

Mata JM, Cáceres J, Lucaya X (1991) CT diagnosis of isolated systemic supply to the lung: a congenital broncho-pulmonary vascular malformation. Eur J Radiol 13:138–142
Mata JM, Cáceres J, Castañer E, Gallardo X, Andreu J (2000) The dysmorphic lung: imaging findings. Postgrad Radiol 20:3–15
McAdams HP, Kirejczyk WM, Rosado-de-Christenson ML, Matsumoto S (2000) Bronchogenic cyst: imaging features with clinical and histopathologic correlation. Radiology 217:441–446
Medelli J, Lattaignant JC, Bertoux JP, Goudot B, Remond A (1979) L'atrésie bronchique segmentarie. Poumon 35:53–58
Murphy JJ, Blair GK, Fraser GC et al (1992) Rabdomyosarcoma arising within congenital pulmonary cysts: report of three cases. J Pediatr Surg 27:1364–1367
Naidich DP, Rumancick WM, Ettenger NA et al (1988) Congenital anomalies of the lung in adults: MR diagnosis. Am J Roentgenol 151:13–19
Nakata H, Egashira K, Warnanake H (1993) MRI of bronchogenic cysts. J Comput Assist Tomogr 17:267–270
Nazarian M, Currarino G, Webb WR, Willis K, Kiphart RJ, Wilson HE (1971) Accessory diaphragm: report of a case with complete physiological evaluation and surgical correction. J Thorac Cardiovasc Surg 61:293
Newman B (2006) Congenital bronchopulmonary foregut malformations: concepts and controversies. Pediatr Radiol 36:773–791
Newman B, Gondor M (1997) MR evaluation of right pulmonary agenesis and vascular airway compression in pediatric patients. Am J Roentgenol 168:55–58
Osborne J, Masel J, McCredie J (1989) A spectrum of skeletal anomalies associated with pulmonary agenesis: possible neural crest injuries. Pediatr Radiol 19:425–432
Partridge JB, Osborne JM, Slaughter RE (1988) Scimitar etcetera: the dysmorphic lung. Clin Radiol 39:11–19
Patcher MR, Lattes R (1963) Mediastinal cysts: a clinicopathologic study of twenty cases. Dis Chest 44:416–422
Paterson A (2005) Imaging evaluation of congenital lung abnormalities in infants and children. Radiol Clin North Am 43:303–323
Pedersen ML, LeQuire MH, Spies JB, Ladd WA (1988) Computed tomography of intralobar bronchopulmonary sequestration supplied from the renal artery. J Comput Assist Tomogr 12:874–875
Pryce DM (1946) Lower accessory pulmonary artery with intralobar sequestration of lung, report of seven cases. J Pathol Bacteriol 58:457–467
Pryce DM, Holmes Sellors T, Blair LG (1947) Intralobar sequestration of lung associated with an abnormal pulmonary artery. Br J Surg 35:18–29
Pugatch RD, Gale ME (1983) Obscure pulmonary masses: bronchial impaction revealed by CT. Am J Roentgenol 141:909–914
Pulpeiro JR, López I, Sotelo T, Ruiz JC, García-Hidalgo E (1987) Congenital cystic adenomatoid malformation of the lung in a young adult. Br J Radiol 60:1128–1130
Recio Rodríguez M, Martínez de Vega V, Cano Alonso R, Carrascoso Arranz J, Martínez Ten P, Pérez Pedregosa J (2012) MR imaging of thoracic abnormalities in the fetus. Radiographics 32(7):E305–E321
Reed JC, Sobonya RE (1975) RCP from the AFIP. Radiology 117:315–319
Rees S (1981) Arterial connections of the lung. Clin Radiol 32:1–15
Remy-Jardin M, Remy J, Ribet M, Gosselin B (1989) Bronchial atresia: diagnostic criteria and embryologic considerations. Diagn Interv Radiol 1:45–51
Restrepo S, Villamil MA, Rojas JC (2004) Association of two respiratory congenital anomalies: tracheal diverticulum and cystic adenomatoid malformation of the lung. Pediatr Radiol 34:263–266
Rogers LE, Osmer JC (1964) Bronchogenic cyst. A review of 46 cases. Am J Roentgenol 91:273–283
Rosado-de-Christenson M, Stocker JT (1991) Adenomatoid malformation. Radiographics 11:865–886
Rosado-de-Christenson M, Frazier AA, Stocker JT, Templenton PA (1993) Extralobar sequestration: radiologic-pathologic correlation. Radiographics 13:425–441
Samuel M, Burge DM (1999) Management of antenatally diagnosed pulmonary sequestrations associated with congenital cystic adenomatoid malformation. Thorax 54:701–706
Savic B, Birtel FJ, Tholen W, Funke HD, Knoche R (1979) Lung sequestration: report of seven cases and review of 540 published cases. Thorax 34:96–101
Senac MO, Wood BP, Isaacs H, Weller M (1991) Pulmonary blastoma: a rare childhood malignancy. Radiology 179:743–746
Stern EJ, Webb WR, Warnock ML et al (2000) Bronchopulmonary sequestration: dynamic, ultrafast, high-resolution CT evidence of air trapping. Am J Roentgenol 74:235–241
Stocker JT (2002) Congenital pulmonary airway malformation: a new name and an expanded classification of congenital cystic adenomatoid malformation of the lung. Histopathology 41(suppl): 424–431
Stocker JT, Kagan-Hallet K (1979) Extralobar pulmonary sequestration. Analysis of 15 cases. Am J Clin Pathol 72:917–925
Stocker JT, Madewell JE, Drake RM (1977) Congenital cystic adenomatoid malformation of the lung. Hum Pathol 8:155–171
Ueda K, Gruppo R, Unger F, Martin L, Bove K (1977) Rhabdomyosarcoma of the lung arising in congenital cystic adenomatoid malformation. Cancer 40:383–388
Vyas HV, Greenberg B, Krishnamurthy R (2012) MR imaging and CT evaluation of congenital pulmonary vein abnormalities in neonates and infants. Radiographics 32:87–98
Ward S, Morcos SK (1999) Congenital bronchial atresia. Presentation of three cases and a pictorial review. Clin Radiol 54:144–148
Wasilewska E, Lee EY, Eisenberg RL (2012) Unilateral hyperlucent lung in children. AJR Am J Roentgenol 198:400–414
West MS, Donaldson JS, Shkolnik A (1989) Pulmonary sequestration. Diagnosis by ultrasound. J Ultrasound Med 8:125–129
Wille L, Holthusem W, Willich E (1975) Accessory diaphragm: report of 6 cases and a review of the literature. Pediatr Radiol 4:14–20
Winters WD, Effmann EL (2001) Congenital masses of the lung: prenatal and postnatal imaging evaluation. J Thorac Imaging 16:196–206
Winters WD, Effmann EL, Nghiem HV et al (1997) Disappearing fetal lung masses: importance of postnatal imaging studies. Pediatr Radiol 27:535–539
Woodring JH, Howard TA, Kanga JF (1994) Congenital pulmonary venolobar syndrome revisited. Radiographics 14:349
Yu H, Li HM, Liu SY, Xiao XS (2010) Diagnosis of arterial sequestration using multidetector CT angiography. Eur J Radiol 76:274–278
Zumbro GL, Green DC, Brott W, Tresaure RL (1974) Pulmonary sequestration with spontaneous intrapleural hemorrhage. J Thorac Cardiovasc Surg 68:673–674